Received: 13 March 2020 | Revised: 16 July 2020 | Accepted: 17 July 2020 | Published on: 30 July 2020

DOI: 10.1002/joc.6761

RESEARCH ARTICLE

International Journal of Climatology RMetS

A sensitivity analysis of the different setups of the RegCM4.5 model for the Carpathian region

Tímea Kalmár[1] | **Ildikó Pieczka**[1] | **Rita Pongrácz**[1,2]

[1]Department of Meteorology, Faculty of Science, Institute of Geography and Earth Sciences, Eötvös Loránd University, Budapest, Hungary

[2]Faculty of Science, Excellence Center, Eötvös Loránd University, Martonvásár, Hungary

Correspondence
Tímea Kalmár, Department of Meteorology, Faculty of Science, Institute of Geography and Earth Sciences, Eötvös Loránd University, 1117 Budapest, Pázmány Péter sétány 1/A, Hungary.
Email: kalmartimea@caesar.elte.hu

Funding information
Hungarian Ministry of Human Capacities under the ELTE Excellence Program, Grant/Award Number: 783-3/2018/FEKUTSRAT; Hungarian National Research, Development and Innovation Fund, Grant/Award Numbers: K-120605, K-129162; Széchenyi 2020 programme, The European Regional Development Fund and the Hungarian Government, Grant/Award Number: GINOP-2.3.2-15-2016-00028

Abstract

The current study focuses on the RegCM4.5 model and specifically on a comparison of hydrostatic and non-hydrostatic approaches as well as on different microphysical parameterisations and planetary boundary layer (PBL) schemes. The main goal of the paper is to simulate the historical regional precipitation characteristics of the Carpathian region as reliably as possible. For this purpose, seven different model experiments at a 10 km horizontal resolution were completed for a 10-year period (1981–1990) using ERA-Interim reanalysis data (with 0.75° resolution) as initial and boundary conditions. Our simulation matrix consists of hydrostatic and non-hydrostatic runs together with different treatments of moisture, namely, the SUBEX and the NogTom schemes. In addition, two PBL schemes are tested, the Holtslag and the UW-PBL scheme. In this detailed validation study, RegCM outputs (e.g., temperature, global radiation, cloud cover, precipitation) are compared to the homogenized, gridded CarpatClim data (available with 0.1° resolution) that are based on measurements at regular meteorological station sites. The validation considers seasonal and monthly means, as well as extreme climatic events. On the basis of the results we can conclude that the role of the non-hydrostatic core can be clearly recognized for precipitation, particularly over mountains. Moreover, it was also found that the UW-PBL scheme performs with a negative bias regarding atmospheric boundary layer thickness and temperature and it reduces the wet/dry biases of the Holtslag PBL scheme. Regarding microphysical schemes, the NogTom scheme performs better than the SUBEX scheme, but the modified SUBEX (SUB4.3) can also reduce the precipitation over mountainous areas.

KEYWORDS

air temperature, global radiation, hydrostatic vs. non-hydrostatic approach, large-scale precipitation schemes, planetary boundary layer schemes, precipitation, regional climate model, total cloud cover

1 | INTRODUCTION

Model-based projections of climate change impacts across multiple sectors suggest that the Carpathian region (located in eastern-central Europe) will be among the hotspot regions with the highest number of severely affected areas in Europe (Ceglar *et al*., 2018). In recent decades, an increase in the frequency and severity of extreme events, such as drought (Spinoni *et al*., 2013), extreme precipitation (Stadtherr *et al*., 2016) and heatwave (Spinoni *et al*., 2015a; Croitoru *et al*., 2016) are observed in the Carpathian region. Because of the special orography of the Carpathians, the basin effects are manifold and they cause many different site-specific phenomena, for example, a stable boundary layer in winter, rain shadows, or temperature inversions (Spinoni *et al*., 2013). Thus, the heterogeneity of the target region justifies the high resolution in regional climate model applications (Giorgi *et al*., 2016b).

Regional climate is determined by the interactions between planetary processes and large-to-local-scale processes. Planetary and synoptic scale processes are well represented in global climate models (GCMs) that use a horizontal resolution in the order of magnitude of 100 km in century-long simulations. Regional climate models (RCMs) are then used for dynamical downscaling to increase the resolution of climate information consistently with the large-scale circulation provided by the driving GCM or reanalysis data. RCMs are also widely used to provide projections on how the climate may change locally through representing land surface heterogeneity with great details and reproducing fine-scale processes more realistically (Flato *et al*., 2013). The analysis of any RCM projection starts with the evaluation of the model simulations of past conditions against the observations (i.e., reference data) for different regions, and then the testing of the model sensitivity with respect to the parameterisations of important physical processes (e.g., cloud formation and development, radiative processes).

Precipitation is one of the most important climate variables, and it is still a great challenge for climate models to realistically simulate the regional patterns, temporal variations, and intensity of precipitation (Kotlarski *et al*., 2014; Gibba *et al*., 2019). The difficulty arises from the complexity of precipitation processes within the atmosphere stemming from cloud microphysics, cumulus convection, large-scale circulations, PBL processes, and many others. Errors in simulated precipitation fields often indicate deficiencies in the representation of these physical processes in the model. It is therefore a primary goal to analyse precipitation for model evaluation and development.

A great number of sensitivity analyses has been completed with the RegCM (Regional Climate Model, available from the International Centre for Theoretical Physics, ICTP) regarding the selection of a suitable integration domain, an adequate horizontal resolution, potential driving models, applied physics schemes, and adaptation tools (Giorgi *et al*., 2003; Sinha *et al*., 2013; Güttler *et al*., 2014; Pieczka *et al*., 2017). More specifically, Giorgi *et al*. (2003) showed and discussed the subgrid surface configuration to be especially useful in improving the simulation regarding the surface hydrological cycle in mountainous regions. In order to evaluate the applicability of RegCM3 to simulate the Asian summer monsoon conditions, a detailed sensitivity analysis of the different cumulus convection schemes was carried out for three different monsoon seasons by Sinha *et al*. (2013). The main finding of the sensitivity analysis of Pieczka *et al*. (2017) is that RegCM4.3 is the most sensitive to the applied convection scheme among the analysed factors (e.g., convective scheme, closure assumption and subgridding method). The effect of the closure assumption related to the convective parameterisation used is secondary, while the use of subgridding has even less influence in the Carpathian region. The validation results of Pieczka *et al*. (2017) for temperature and precipitation suggest that the overall best performance for the Carpathian region is achieved when using the mixed Grell-Emanuel scheme (Emanuel, 1991; Grell, 1993; Emanuel and Živković-Rothman, 1999) together with Fritsch and Chappell (Fritsch and Chappell, 1980) closure.

Another key factor that can lead to changes in the climatic parameters is the planetary boundary layer (PBL). PBL processes control near-surface temperature and precipitation. Ground can be heated or cooled by modifications in the boundary layer. Both stable and unstable conditions of the boundary layer have an important role in wind speed (Burk and Thompson, 1989). Güttler *et al*. (2014) investigated how two PBL parameterisation schemes (Holtslag (Holtslag *et al*., 1990) PBL scheme and University of Washington (UW) PBL scheme described in Bretherton *et al*. (2004)) performed in RegCM4.2. The study showed the advantage of the UW-PBL scheme in regions where significantly warm and moderately dry biases are present. Velikou *et al*. (2019) found similar results about the effect of the UW-PBL scheme: it produces a negative bias in atmospheric boundary layer thickness, which is connected to the intensity of surface heating and the evaporated amount of water in the air.

The current study fits into the above series of analyses with the novelty of evaluating the impact of different dynamical core (hydrostatic and non-hydrostatic) and parameterisation schemes (such as large-scale

precipitation scheme and PBL scheme) on model performance. The RegCM4.5, which was used for this study, has been available online since 2016 and includes two main improvements: (a) the possibility to use a non-hydrostatic dynamical core; and (b) an additional new microphysics scheme (Elguindi *et al*., 2014). The main aim of this study is to evaluate these improved elements of RegCM for the Carpathian region and to simulate the historical regional precipitation characteristics as reliably as possible and find the best configuration for future climate projections.

The paper is organized as follows: first, we provide a brief description of the model version used in the study and the most relevant parameterisation schemes. Then, we summarize the main features of model experiments and validation data. Furthermore, a newer comprehensive index, namely, the Distance between Indices of Simulation and Observation (DISO) is presented for detailed validation. Results are shown and evaluated in Section 3, followed by a summary and conclusions in Section 4.

2 | MODEL, DATA AND METHODOLOGY

2.1 | Model description

The climate model RegCM originally stems from the National Center for Atmospheric Research/Pennsylvania State University (NCAR/PSU) Mesoscale Model version MM4 (Dickinson *et al*., 1989; Giorgi, 1989), now maintained at the ICTP. The RegCM4.5 is based on the dynamics of NCAR MM5 (Grell *et al*., 1994). One of the main improvements in this version is that the model can use a non-hydrostatic dynamical core, which allows small horizontal resolutions of the order of a few kilometres or even less. A full description of the model equations and possible parameterisations available in version 4.5 can be found in detail in Elguindi *et al*. (2014). We used the Biosphere-Atmosphere Transfer Scheme (BATS) to describe the role of vegetation and interactive soil moisture in modifying the surface-atmosphere exchanges of momentum, energy, and water vapour (Dickinson *et al*., 1993). The convective precipitation parameterisations used in this study are the Grell (1993) scheme over land and the MIT-Emanuel scheme (Emanuel, 1991) over sea. The turbulent transports of sensible heat, momentum and water vapour in the PBL over land and ocean are calculated using the scheme developed by Holtslag *et al*. (1990), which permits non-local transport in the convective boundary layer. As an alternative to the Holtslag scheme, the turbulence closure model of the UW (Bretherton *et al*., 2004) was coupled to the RegCM. The implementation of this UW scheme in RegCM4 is documented in O'Brien *et al*. (2012) and the initial comparisons between the two PBL schemes are described in Giorgi *et al*. (2012), and Güttler *et al*. (2014). Different resolved-scale cloud microphysics schemes are built in the model version 4.5, for example, the Subgrid Explicit Moisture Scheme (SUBEX, Pal *et al*., 2000) and a new cloud microphysics scheme (called NogTom, Nogherotto *et al*., 2016).

In the earlier RegCM versions, the resolved-scale cloud physics are treated by the SUBEX, which calculates fractional cloud cover as a function of grid point average relative humidity and includes only one prognostic equation for cloud water. Rain is calculated diagnostically from the cloud liquid: it forms when the in-cloud liquid water exceeds a temperature-dependent threshold (Sundqvist *et al*., 1989). Unlike in the NogTom scheme, the ice and snow phases are not treated directly in this scheme. Furthermore, the SUBEX includes the evaporation and accretion processes for precipitation.

The NogTom scheme is a new parameterisation based on a multi-phase one-moment cloud microphysics scheme built upon the implicit numerical framework recently developed and implemented in the ECMWF Integrated Forecasting System (IFS) (Tiedtke, 1993; Tompkins *et al*., 2007). The parameterisation solves five prognostic equations for water vapour, cloud liquid water, rain, cloud ice, and snow mixing ratios. Compared to the pre-existing SUBEX scheme, it allows proper treatment of mixed-phase clouds and a more realistic physical representation of cloud microphysics. In addition, the NogTom scheme yields improved cloud field simulation and in particular it removes the overestimation of the upper level cloud characteristics of the SUBEX scheme. This new cloud microphysics scheme is described in detail in Nogherotto *et al*. (2016).

2.2 | Simulations

Simulations were carried out for the target period 1980–1990 with initial and lateral boundary conditions from the 0.75° horizontal resolution ERA-Interim data (Dee *et al*., 2011) at a 10-km horizontal resolution in order to represent the fine topography of the target area (Gao *et al*., 2006). The resolution of 10 km was chosen to allow both hydrostatic and non-hydrostatic approaches in the simulations. Furthermore, the validation database (CarpatClim) has similar resolution as the simulations. The first year, 1980 was selected as a spin-up to ensure that all components of the regional climate model reach physical equilibrium under the applied forcing, and the results for the decade 1981–1990 were analysed. This

decade was selected as a result of compromise to complete as many simulations as possible for comparison on the one hand, and being long enough for climatic analysis (WMO, 2007) on the other hand. The period 1981–1990 is the first decade of the current climatic normal (1981–2010), and was used in earlier studies (e.g., Pieczka *et al*., 2017).The integration domain is over 6°–29°E and 43.8°–50.6°N (thus the grid contains 231 × 69 cells) after removing the buffer zones (Figure 1). The buffer zone at the outer boundaries of the model was set to 24 grid points with exponential relaxation. This domain was defined to include the Carpathian Basin and surrounding areas, thus, the main topographical features of the domain, such as the Carpathians enclosing the basin in the east, the Alps to the west, the Dinarides to the south, and a small fraction of the Adriatic Sea are represented. The dominant wind direction over the basin is west-northwest (Bihari *et al*., 2018), resulting in a west-to-east spatial gradient of precipitation modulated by local topography. As the air masses from the Atlantic region cross large mountain ranges such as the Alps, which behave as an orographic barrier, the contribution of this source to the precipitation decreases towards the east. The main relevant properties of the simulations are shown in Table 1. Our simulation matrix contains seven different model simulations: the RegCM4.5 was run both in hydrostatic and non-hydrostatic mode with different large-scale precipitation schemes (i.e., SUBEX, modified SUBEX – SUB4.3, and NogTom) and PBL schemes (Holtslag and UW).

Four simulations were defined from the combination of the different dynamical cores and large-scale precipitation schemes: H_SUBEX, NH_SUBEX, H_NogTom, NH_NogTom. An additional simulation (NH_NogTom_NC) uses non-hydrostatic dynamics and the NogTom scheme, but convective parameterisation is switched off over land and the deep convection is resolved explicitly. For the SUBEX scheme, we also used a modified version called SUB4.3 during the testing (in H_SUB4.3). The main differences between the SUBEX and SUB4.3 are that (a) the cloud-to-rain autoconversion rate was decreased from 0.0005 to 0.00025 s^{-1}, (b) the raindrop evaporation rate coefficient was increased from $0.2{\cdot}10^{-4}$ to $1{\cdot}10^{-3}(kg{\cdot}m^{-2}{\cdot}s^{-1})^{-1/2}{\cdot}s^{-1}$, and (c) the raindrop accretion rate was decreased from 6 to 3 $m^3{\cdot}kg^{-1}{\cdot}s^{-1}$ in SUB4.3 (Torma *et al*., 2011). These modified parameters help to decrease the overestimation of precipitation and were built into the RegCM4.3 as default values (Elguindi *et al*., 2011), but were changed back to the previous values in the RegCM4.5. We completed two additional simulations (namely H_SUB4.3_UW and H_NogTom_UW) that use the UW-PBL scheme instead of the Holtslag scheme, because the planetary boundary layer plays an important role in the formation of winter inversion and previous studies (e.g., Güttler *et al*., 2014) showed improvement in reducing temperature biases with UW scheme. Although H_NogTom_UW was completed, Giorgi *et al*. (2016a) revealed problems in the interaction between the NogTom and UW-PBL schemes; therefore, this simulation is not included in the current study.

2.3 | Methodology

A comprehensive assessment of these simulations is important to identify their different overall performances, such as the accuracy of simulated variables against observed fields. For the purpose of validation, we used the corresponding time period (1981–1990) from the

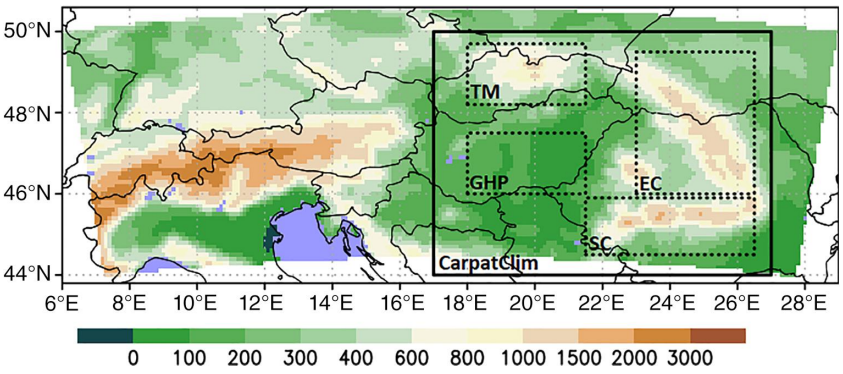

FIGURE 1 The topography (m) of the integration (after removing the buffer zones) domain for the RegCM4.5 simulations. Validation is shown for the eastern half of the RegCM integration domain covering the CarpatClim domain (indicated by a solid rectangle on the map). In addition, four special geographical subregions with different orographic and climatic conditions are selected for more detailed validation: The dotted rectangles indicate the Tatra Mountains (TM), Eastern Carpathians (EC), Southern Carpathians (SC) and Great Hungarian Plain (GHP)

TABLE 1 The main settings of the RegCM4.5 simulations analysed

	Dynamics	Large-scale precipitation	PBL	Cumulus convection – land/ocean
H_SUB4.3	Hydrostatic	Modified SUBEX – SUB4.3	Holtslag	Grell/MIT-Emanuel
H_SUB4.3_UW	Hydrostatic	Modified SUBEX – SUB4.3	UW	Grell/MIT-Emanuel
H_SUBEX	Hydrostatic	SUBEX	Holtslag	Grell/MIT-Emanuel
NH_SUBEX	Non-hydrostatic	SUBEX	Holtslag	Grell/MIT-Emanuel
H_NogTom	Hydrostatic	NogTom	Holtslag	Grell/MIT-Emanuel
NH_NogTom	Non-hydrostatic	NogTom	Holtslag	Grell/MIT-Emanuel
NH_NogTom_NC	Non-hydrostatic	NogTom	Holtslag	—

TABLE 2 Meteorological variables, units, retrieval methodology and number of stations used

Meteorological variable	Unit	Methodology for retrieving the primary data	Total number of stations used as a basis of interpolation in CarpatClim
Mean temperature	°C	Arithmetical mean from daily minimum and maximum temperature	542 (T_{max} and T_{min})
Precipitation amount	mm	Standard daily measurement	1,165
Cloud cover	Tenth	Computed from 3-hr measurements	498
Global radiation	$MJ \cdot m^{-2}$	Computed from daily sunshine duration measurements	333

CarpatClim database, which is a high-resolution, homogeneous, gridded database for the Carpathian region with a 0.1° horizontal resolution, covering the 1961–2010 period, containing all the major surface meteorological variables (Spinoni *et al*., 2015b). According to Katragkou *et al*. (2015), the role of other climatological parameters – besides temperature and precipitation – should be included in the evaluation procedure of RCMs (e.g., radiative fluxes, sensible and latent heat fluxes and cloud properties) in order to reveal the complex relationships between various local climatic elements. That is why daily temperature, global radiation, cloud cover and precipitation datasets (Table 2) were downloaded, of which monthly and seasonal means were calculated for the validation domain (44°–50°N, 17°–27°E), and compared to the simulated values. In addition, we selected four subregions with different orographic and climatic conditions for detailed validation: the Tatra Mountains (TM), the Great Hungarian Plain (GHP), the eastern part of Carpathian Mountains (EC) and the southern part of Carpathian Mountains (SC) (Figure 1). Since precipitation is a key parameter, our focus is on a range of precipitation metrics, more specifically, mean precipitation climatology, daily precipitation probability density functions (PDFs) and the precipitation bias depending on elevation above sea level. In order to compare the different simulations in each subregion and to understand how well simulations fit each other in terms of correlation, standard deviation, and RMS difference, the Taylor diagrams were produced. Furthermore, a new statistical index (DISO) is used to quantify the performance of the simulations.

2.4 | DISO index

In general, the comprehensive performance of the simulations is quantified by single statistical indices, such as correlation coefficient (r), absolute error (AE), and root-mean-square error (RMSE). Hu *et al*. (2019) developed a new index (DISO) to describe the overall performance of different models or simulations against observation. This new index is a merger of different statistical metrics including r, AE, and RMSE in a three-dimensional coordinate system. For the observed time series ($A = [a_1, a_2,..., a_n]$) and the model-simulated time series ($B = (b_1, b_2,..., b_n)$], the r, AE and RMSE are calculated as follows:

$$r = \frac{\sum_{k=0}^{n} (a_i - \bar{a})(b_i - \bar{b})}{\sqrt{\sum_{k=0}^{n} (a_i - \bar{a})^2} \sqrt{\sum_{k=0}^{n} (b_i - \bar{b})^2}}$$

$$\mathrm{AE}=\frac{1}{n}\sum_{k=0}^{n}(a_i-b_i)$$

$$\mathrm{RMSE}=\frac{1}{n}\sum_{k=0}^{n}\sqrt{(a_i-b_i)^2}$$

where $\bar{a}$ and $\bar{b}$ are the means of A and B, respectively, and n is the length of the time series. In order to eliminate the influence of dimensions, AE and RMSE are normalized (divided by the absolute observation mean ($|\bar{a}|$)). DISO is then defined as:

$$\mathrm{DISO}=\sqrt{(r-1)^2+\mathrm{NAE}^2+\mathrm{NRMSE}^2}$$

where N indicates normalized values of AE and RMSE. The simulation is close to the observation, when DISO is close to 0.

The advantage of using DISO against the Taylor diagram is that the comprehensive performances of the different models are still not quantified in the latter (Hu *et al.*, 2019). Taylor diagram was developed with the combination of three statistical metrics: the standard deviation (*SD*), correlation coefficient (r) and the centred RMS difference (RMSD).The diagram determines which percentage of the RMSE can be attributed to the difference in variance and how much is due to the poor pattern similarity (Taylor, 2001). Contrary to this, the DISO index uses a slightly different concept by providing a single statistical index value (which is the combination of r, AE and RMSE), and hence it enables us to determine the rank of performance and summarize the overall evaluation of individual simulations. However, according to Xu and Han (2019), a single index cannot show the differences between the simulations explicitly and it loses the detailed information. In order to have a better understanding of the DISO index, a comparison of the new index and Taylor diagram was conducted and discussed in the paper. We found that in our case both methods agreed about which simulation is the closest to the observations.

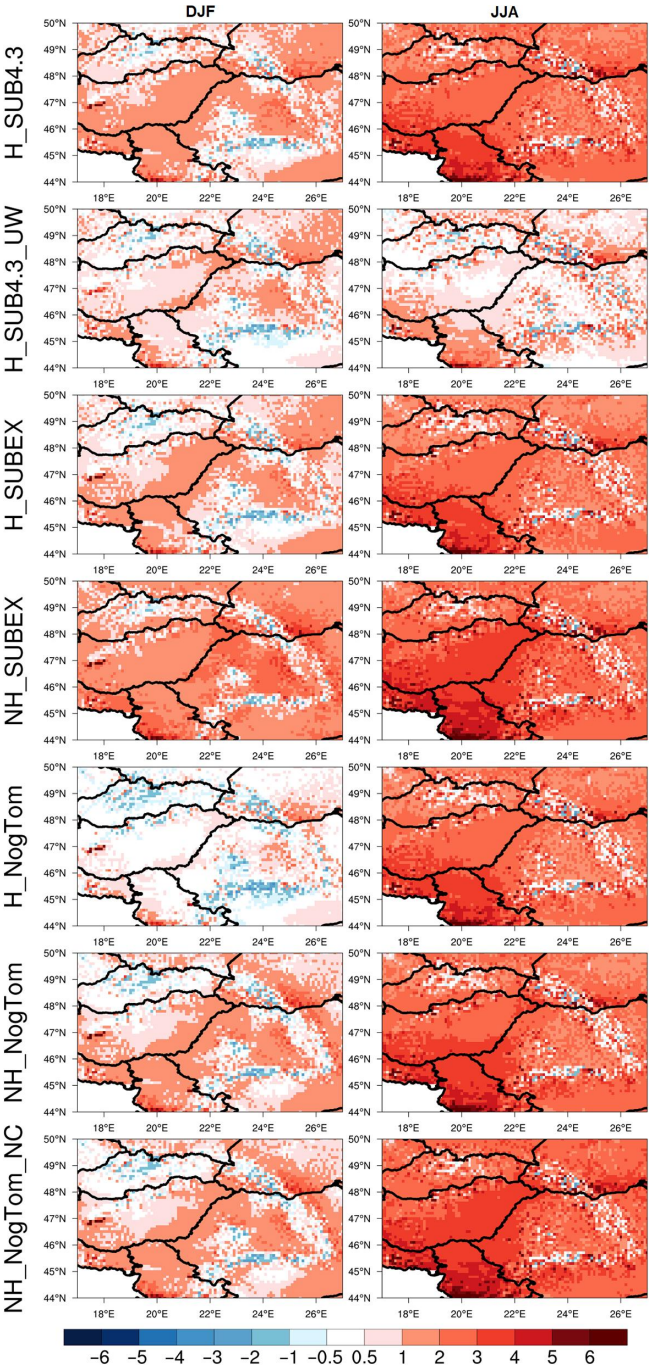

FIGURE 2 The winter (left) and summer (right) average temperature bias (°C) of 10-km horizontal resolution RegCM simulations, 1981–1990 (validation data: CarpatClim)

3 | RESULTS AND DISCUSSION

In this section, we evaluate the RegCM4.5 by comparing different model runs with the CarpatClim data set and sounding data. We analyse not only precipitation and temperature, but also global radiation and cloud cover. The presented sensitivity study includes different temporal scales (seasonal, monthly and daily). In order to demonstrate the effect of the two PBL schemes, we compare our simulations (only H_SUB4.3 and H_SUB4.3_UW) with sounding data (downloaded from the Integrated Global Radiosonde Archive [IGRA]) in two different weather conditions (during a cold air pool in December 1986 and a heatwave in July 1987) over Budapest (47.4°N, 19.2°E).

3.1 | Temperature

Figure 2 shows the winter (DJF) and summer (JJA) mean near-surface temperature bias with respect to CarpatClim over the Carpathian region averaged over the time period 1981–1990. The main differences between RegCM4.5 simulations can be found in winter: the use of the SUBEX scheme overestimates temperature over lowlands compared to other simulations, while the NogTom scheme produces the smallest biases over Hungary. Comparing the two PBL schemes, the UW scheme has better results for the temperature biases. In general, all simulations have negative biases over the Carpathian mountain ridge, the largest (between −1°C and −2°C) being with the NogTom scheme. In winter the Lake Balaton appears with a strong positive temperature bias in all RegCM4.5 simulations. This can be explained by the fact that the RegCM developers changed the interpolation algorithm (RegCM4.3 uses bicubic interpolation, whereas RegCM4.5 uses bilinear interpolation), which caused the surface cover to change. Thus, differently from RegCM4.3, the Lake Balaton appears as a water surface in RegCM4.5 where the model uses a different parameterisation scheme (i.e., cumulus convection parameterisation) from the schemes over the land surfaces. In addition, the CarpatClim is a homogenized, gridded dataset that does not contain any measurement above the water surface, therefore the water surface results in greater positive bias values relative to the erroneous reference data representing only land area.

The spatially averaged mean temperature bias for summer is around 4°C for the entire domain (the summer bias is especially great in southern Serbia), except when we applied the UW-PBL scheme, where the bias is reduced to 1–2°C. This could be related to the fact that the UW-PBL scheme increases the cloud cover, and thus, reduces net surface shortwave flux resulting in a decrease of the near-surface temperature errors (Güttler *et al.*, 2014). The signs of seasonal mean bias in the mountains change within short distances, especially when the error is close to zero in summer. This is probably due to the fact that the observation network is not as dense in these areas as our grid resolution, so the reference data may involve higher uncertainty (related mainly to the orientation of slopes) than the simulated data. The effect of the non-hydrostatic core is not observed in the temperature bias fields. The spatial distributions of bias fields show that the minimum values occur over the mountains, while the highest biases appear in the southern part of the domain (in Serbia).

The annual cycle of temperature bias is shown over the subregions in Figure 3. Every simulation resulted in the highest bias values (~3°C – except H_SUB4.3_UW, which is 1–2°C) in summer. This warm (and dry) bias is presented in simulations performed with other models (Christensen *et al.*, 2008; Bucchignani *et al.*, 2016) as well

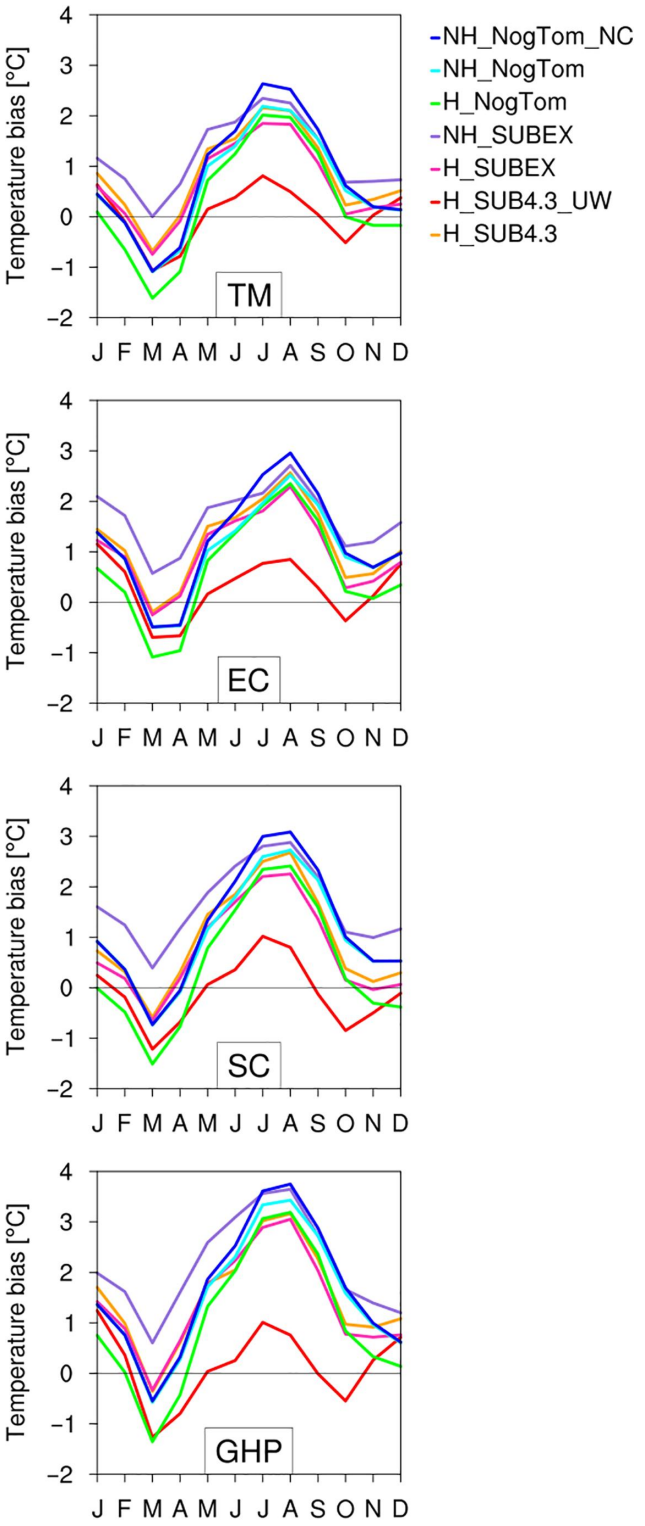

FIGURE 3 The annual mean temperature bias (°C) of RegCM simulations over the subregions, 1981–1990 (validation data: CarpatClim)

as RegCM simulations (Pieczka *et al.*, 2017; Velikou *et al.*, 2019) in general. In winter the positive biases of NH_SUBEX appear over all subregions. In summer the simulations using a non-hydrostatic core produce higher positive biases, but the differences between NH and H are not substantial. The differences of temperature bias between the H_SUB4.3_UW and other simulations are around 2°C. The H_SUB4.3_UW performs the best in the case of temperature over the subregions, because both the overestimation in summer (in the right column of Figure 2) and the negative bias in spring (not shown here) are reduced compared to the other simulations. This could be connected with the better representation of cloud cover. We can conclude that this simulation has the lowest bias compared to the CarpatClim.

For a more detailed validation, the area-averaged monthly mean temperature values are compared to the CarpatClim database for the subregions in Figure 4. In general, the simulations overestimate the lower temperature values (i.e., <0°C). The H_NogTom has the best performance, while the NH_SUBEX has the highest values in this interval below freezing. Between 0°C and 15°C the simulations are closer to the observation, but the simulations that use the SUB4.3 or NogTom large-scale precipitation schemes underestimate the CarpatClim. Above 15°C, the overestimation of simulations increases and reaches 3–4°C, except the H_SUB4.3_UW, which captures the values of CarpatClim very well. The simulations using a non-hydrostatic core have the largest positive bias in all the subregions, which can be seen in Figures 2 and 3, too. This highlights the fact that the current setups are not yet fully appropriate and further testing of the non-hydrostatic approach within RegCM is needed in the future.

We also analysed the vertical temperature profiles of H_SUB4.3 and H_SUB4.3_UW, because the difference between these simulations is only in the form of application of the PBL scheme. For the validation, we used sounding data over Budapest (19°E, 47.5°N) in two different weather conditions (Figure 5). The first case is a cold air pool situation in winter 1986 (the longest occurred within 1981–1990), which is a relatively frequent phenomenon in the Carpathian basin causing severe pollution problems in urban areas. The theory of cold air pool formation in valleys and basins (Geiger, 1951) highlights the role of longwave radiation loss and the downward flux of sensible heat from the overlying atmosphere to counter this loss. A cold air pool usually appears when an anticyclone builds up after a cold front passes over the basin, and it is usually eliminated by a strong cold front of new mid-latitude cyclone (Daly *et al.*, 2009). Vertical profiles at 0 UTC for 4 days in winter are shown from 300 m to 1,000 m in Figure 5a, where inversion is the most intense on these days. The plot shows that both simulations overestimate the measured temperature values along the profiles, especially in the lower levels, so the

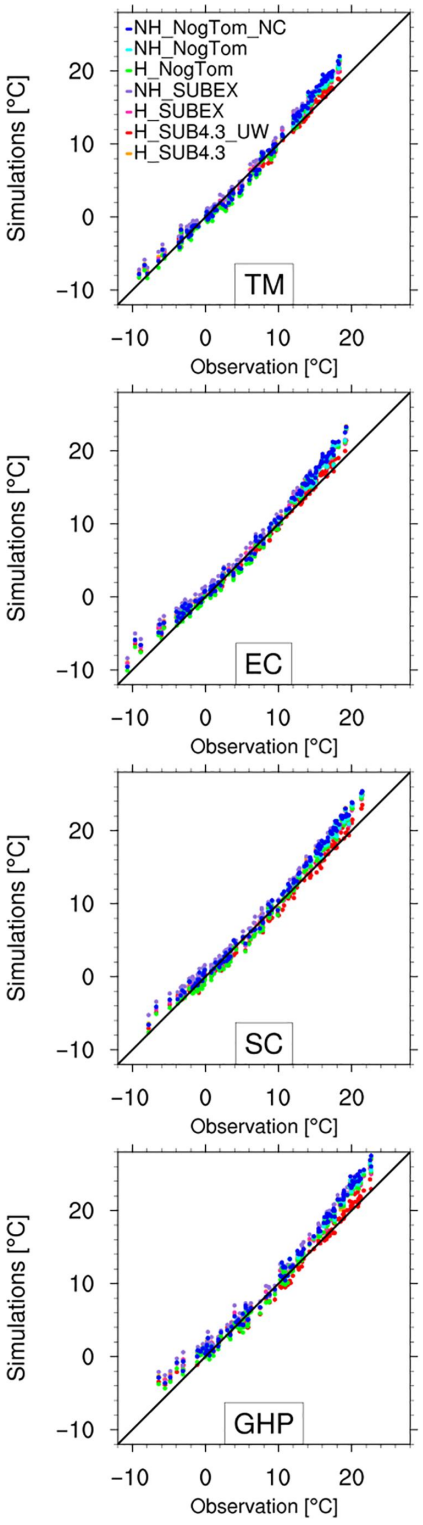

FIGURE 4 The monthly simulated temperature values (y axis) compared to the observation data (CarpatClim, x axis) for the four subregions, 1981–1990

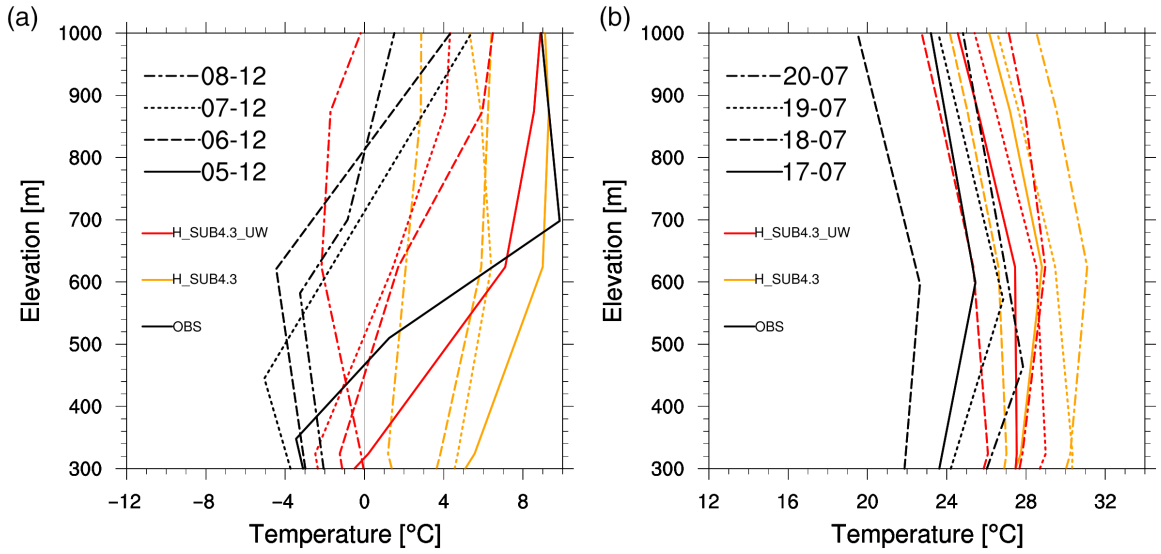

FIGURE 5 Temperature vertical profiles in Budapest (47.5°N, 19°E) in winter days at 0 UTC (5–8 December 1987, [a]) and summer days at 12 UTC (17–20 July 1987, [b]) (data source: IGRA)

extent of inversion is generally smaller than in the radiosonde measurements. The overestimation reaches 6°C with the default scheme. The largest temperature gradient appears on the first day (4°C/100 m in the first 700 m), but the simulations cannot reproduce this gradient (H_SUB4.3:0.6°C/100 m; H_SUB3.4_UW: 1.3°C/100 m). The vertical profile of ERA-Interim (which was used for forcing) has patterns similar to the sounding data (not shown). In general, the H_SUB4.3_UW seems to be closer to the observations, although it does not capture the overall profile very well. Based on the results of Güttler *et al.* (2014) the UW parameterisation generally reduces lower tropospheric temperatures (possibly due to reduced entrainment of potentially warm, free tropospheric air into the PBL).

In summer, another health-threatening weather situation is selected, namely a heatwave across Europe (in July 1987), which was the strongest event in the decade (Spinoni *et al.*, 2015a). The differences between the simulations and measurements are not so large as in winter (Figure 5b). Similarly to winter, the UW scheme reduces the warm bias compared to the Holtslag scheme in summer, too. This is consistent with the improvements in temperature climatology when compared against CarpatClim over the whole domain, as it can be seen in Figures 2 and 3. Nevertheless, both experiments capture the coolest and warmest days. The vertical temperature gradient is relatively small, approximately −0.2°C/100 m. In summer the simulation results are closer to the observations than in winter, which could be connected to the fact that it is difficult to simulate the cold air pool conditions in general, that is, not only with climate models but also with numerical models used in short range weather forecasts.

3.2 | Global radiation

The primary driver of latitudinal and seasonal variations in temperature is the seasonally varying pattern of incident sunlight, and a fundamental driver of the atmospheric circulation is the local-to-planetary scale imbalance between shortwave and longwave radiation. The impact of the distribution of insolation on temperature can be strongly modified by the distribution of clouds and surface characteristics. In this section we evaluate the global radiation component of RegCM simulations, which are compared to data available from CarpatClim. The limited coverage of global radiation measurements dictated the need to develop models to estimate solar radiation based on other, more readily available data, such as sunshine hours, air temperature, precipitation, relative humidity and cloudiness (Almorox and Hontoria, 2004). The most commonly used variable for estimating global solar radiation is sunshine duration. The main advantages of using sunshine duration include easy measurements, as well as widely available data. For instance, it is used in the CarpatClim project since global radiation is not directly measured at many stations within the region, therefore, in the case where only sunshine duration was available, global radiation was calculated using the equation postulated by Ångström (1924) and modified by Prescott (1940). Observed global radiation was used wherever it was available at station level.

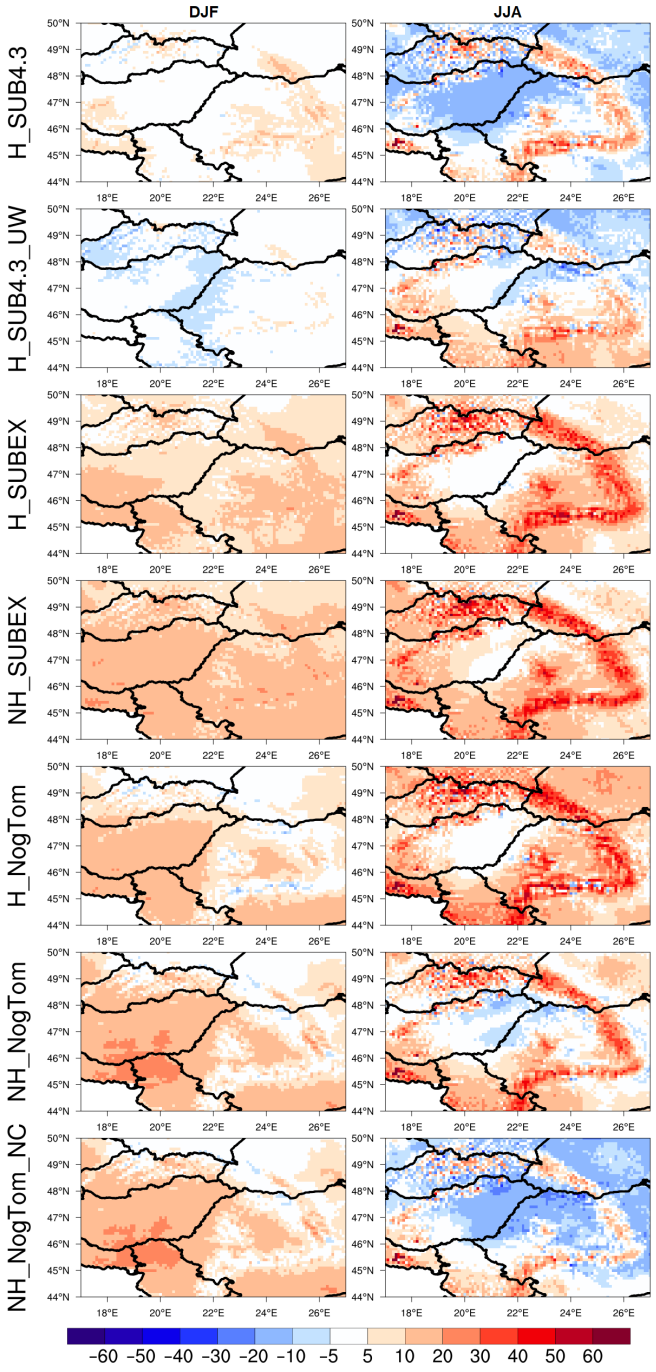

FIGURE 6 The winter (left) and summer (right) average global radiation bias ($W \cdot m^{-2}$) of 10-km horizontal resolution RegCM simulations, 1981–1990 (validation data: CarpatClim)

Seasonal average global radiation from RegCM and CarpatClim data are compared over the Carpathian region in Figure 6. The SUB4.3 precipitation scheme produces the smallest positive biases all over the region in winter, and negative biases appear only with the UW-PBL scheme. The NogTom scheme shows substantial improvements over mountains compared to the SUBEX scheme. In summer the bias characteristics of the experiments are similar to each other, namely, the biggest overestimation can be found over mountains. The modified SUBEX scheme causes negative bias values ($\sim$30 $W \cdot m^{-2}$) over lowlands. It can be connected to the decrease of the cloud-to-rain autoconversion rate, which leads to more clouds that reduce the incoming radiation. No significant differences are found in the bias maps between the SUBEX and NogTom schemes, except NH_NogTom_NC, which shows better results over the Carpathians. During the summer, the observed cloud cover has a more pronounced peak over lowlands compared to the simulations using the NogTom Scheme (10–20%). It will be discussed in more detail in Section 3.3.

3.3 | Cloud cover

Since cloudiness is a key component in the discussion concerning radiation, we compare our model results with cloud cover of the CarpatClim. On the basis of the cloud cover bias maps (Figure 7), every simulation shows underestimation over lowlands in winter. The decrease in cloud cover leads to an increase in incident radiation, inducing an increase in sensible heat flux and warmer surface temperatures. The underestimations are negligibly small with the UW-PBL scheme in winter (from −10% to 10%). The large-scale precipitation schemes do not show huge differences, only the NogTom scheme overestimates (10%) the cloud cover over the mountain ridge. In general, the non-hydrostatic core causes bigger negative bias values over Hungary (around −40%) than the hydrostatic core. These negative biases are probably caused because of the fact that the Holtslag scheme cannot reproduce foggy situations and the stratocumulus clouds properly (O'Brien *et al*., 2012), which are common over this area in winter. Note, however, that winter shortwave radiation absolute amounts are very small over central and northern Europe in winter, so that larger negative relative biases (−40%) in cloud cover over this area correspond to small radiation values, which does not substantially affect the overall energy budget of the surface (as shown in Figure 6, radiation bias in winter is smaller than in summer).

In summer the large-scale precipitation schemes have a major role in cloud formation: the simulations can be separated into two groups. Positive biases appear with the NogTom scheme over lowlands, while the SUBEX scheme underestimates the cloud cover over the entire domain. A possible explanation can be related to the different approach in treating convective detrainment. More specifically, while in the NogTom scheme the

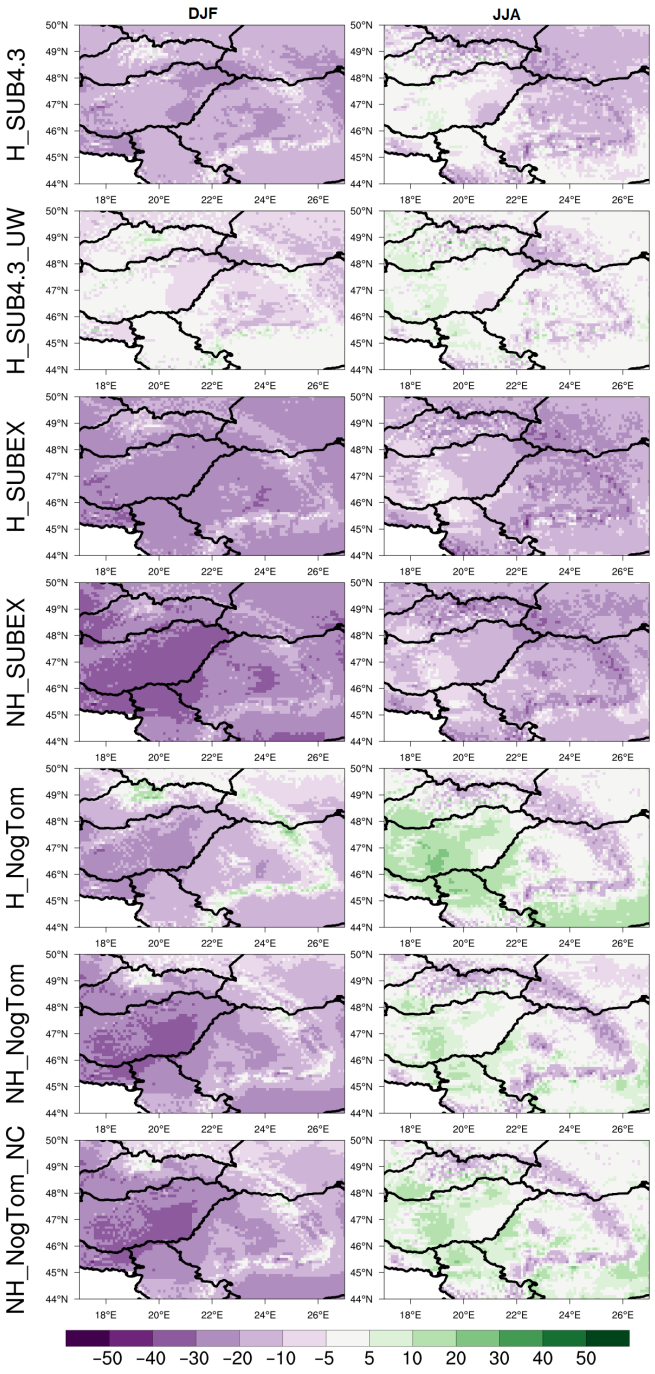

FIGURE 7 The winter (left) and summer (right) average cloud cover bias (%) of 10-km horizontal resolution RegCM simulations, 1981–1990 (validation data: CarpatClim)

detrainment produced by the convection scheme is given as an input to the microphysics scheme and is therefore subjected to microphysical processes, in SUBEX the detrainment is a source of cloud liquid water and is not involved in the formation of rain until the following time step (Nogherotto *et al.*, 2016). The H_SUB4.3 shows the best performance; the biases are between −10% and 10%. It can clearly be seen that the modification of the SUBEX scheme has a positive effect on cloud formation and the simulation of global radiation, too. This pattern is well correlated with the radiation bias discussed in Section 3.2, indicating that cloudiness and radiation biases have opposite signs, as expected.

The greatest amount of cloud cover is in winter over the domain and a secondary maximum appears in the beginning of summer, when the convective season starts (Figure 8). The minimum values appear in July and August, because the anticyclones in summer cause stable conditions with no clouds. All experiments capture well the annual cycle of cloud cover over mountains, but the runs show much lower values in winter over the lowland (the biases are between −20% and − 40%, except for H_SUB4.3_UW). In general, differences between H_SUBEX and NH_SUBEX appear in winter, when the hydrostatic simulation is closer to the observation. The NH_NogTom and NH_NogTom_NC simulations do not show significant differences to each other, implying that the application of a convective scheme does not have a substantial effect on cloud cover. Furthermore, the H_SUB4.3_UW seems better over all subregions, especially in winter compared to the non-hydrostatic simulations. The modification of the SUBEX scheme improves the results, but the general underestimation appears in all months. Substantial differences appear between the H_SUB4.3 and H_SUB4.3_UW simulations since the UW scheme captures the winter values much better, but it somewhat overestimates cloud cover (with 20%) in autumn.

3.4 | Precipitation

Regarding precipitation, the seasonal absolute (left two columns) and relative mean biases (right two columns) are shown in Figure 9. Precipitation evidently depends on elevation; more rain falls in the mountains than in lower elevated regions. The largest positive biases are found over mountains, where the simulations overestimate the precipitation up to 80–100%. Unlike the other simulations, the modified SUBEX scheme reduces the positive precipitation bias over mountainous areas in winter, while the NH_NogTom causes more precipitation over mountains than the SUBEX scheme. This increased precipitation can be connected to the core of the model, because the NH_NogTom_NC simulation does not use a convective precipitation parameterisation scheme and still, its bias pattern is quite similar to other simulations with a NH core (as shown in the first and third column of Figure 9).

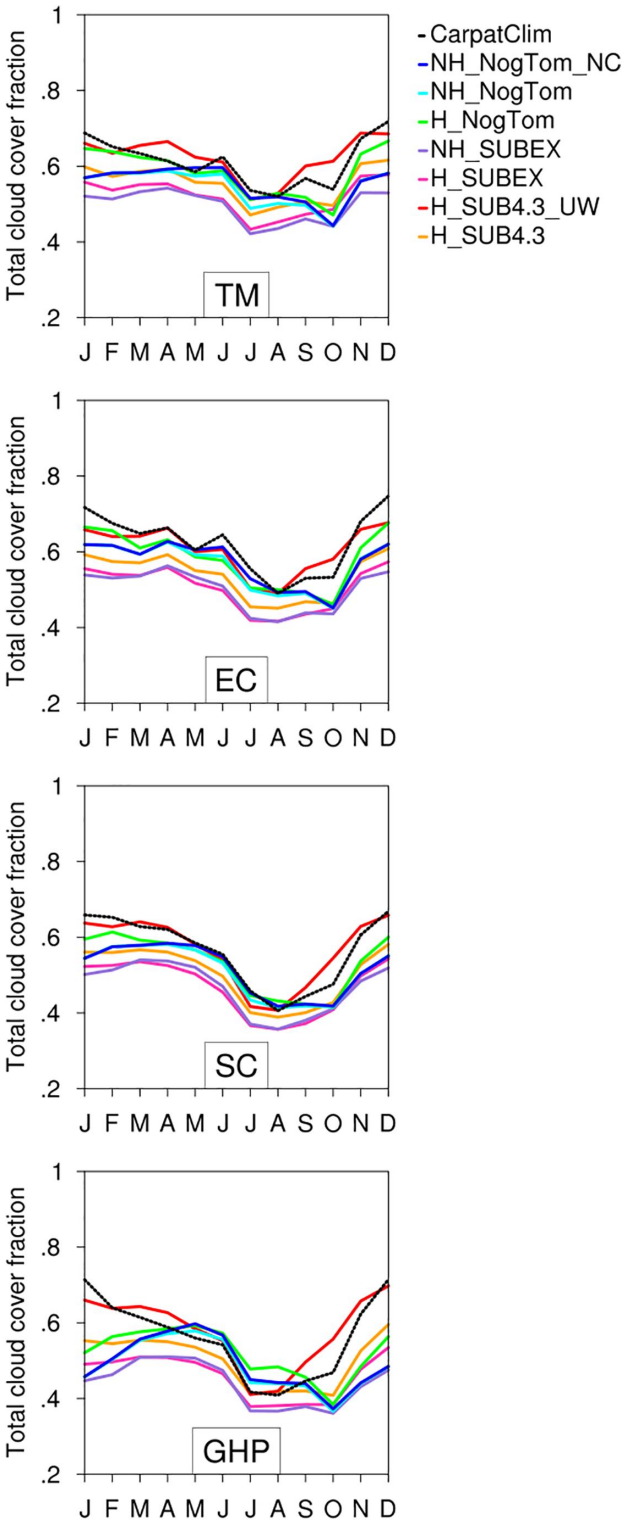

FIGURE 8 Annual cycle of cloud cover fraction over the four subregions, 1981–1990

In winter (when the convective activity in the region is minimal), no substantial differences can be seen between the NH_NogTom and NH_NogTom_NC simulations. Precipitation is overestimated in all seasons over mountains by ∼50%. Compared to the CarpatClim, the H_SUBEX and H_SUB4.3 result in the lowest mean precipitation bias over the GHP. As the mean temperature biases (Figure 2) are different, the precipitation biases of H_SUB4.3 and H_SUB4.3_UW are also quite dissimilar; larger negative biases appear with the H_SUB4.3_UW simulation. More specifically, the UW scheme tends to reduce the rather wet or dry biases of the Holtslag scheme (similar results were shown by Güttler *et al.*, 2014). Comparing the hydrostatic and non-hydrostatic dynamical cores, the latter produced more precipitation over mountains and less over lowlands. Moreover, seasonal mean precipitation bias values for Hungary substantially decreased with the NH_NogTom simulation compared to NH_SUBEX.

In summer the results clearly show that the UW-PBL also affects precipitation as it reduces the precipitation flux in the majority of the study domain, especially over the Carpathians, and negative biases appear too (-1 mm·day^{-1}, -40%). The results of NH_NogTom_NC in summer also substantially differ from the other simulations with the largest negative biases (~ 2 mm·day^{-1}, $\sim 60\%$) over lowlands, while the precipitation bias is positive over mountains. It can be related to the fact that this simulation does not use convective parameterisation and the 10 km horizontal resolution is not fine enough for the model dynamics to appropriately simulate deep convection, but the orographic effect is already manifested at this resolution.

According to Pieczka *et al.* (2017), there are deviations between ERA-Interim and CarpatClim in the case of precipitation, namely, the area east of Hungary is wetter in the reanalysis than in the CarpatClim in each season, while Hungarian grid points are wetter in winter, spring, and autumn but are drier in summer in ERA-Interim. Based on these deviations, the biases partially originate from the initial and lateral boundary conditions.

In order to compare the daily precipitation intensities and to focus more closely on the extremes, we used the normalized PDF of daily precipitation, which is the frequency of occurrence of precipitation events within a certain interval of intensity normalized by the total number of days with at least 1 mm of rainfall, including all grid points in the subregions. In order to carry out a more detailed evaluation of the different configurations of RegCM, a separation of precipitation was performed (considering the fact that total precipitation is calculated as the sum of stratiform and convective precipitation) and the results of this analysis are shown in Figure 10. It is important to note that the CarpatClim does not contain convective and stratiform precipitation categories separately, but only the total precipitation, that is why the

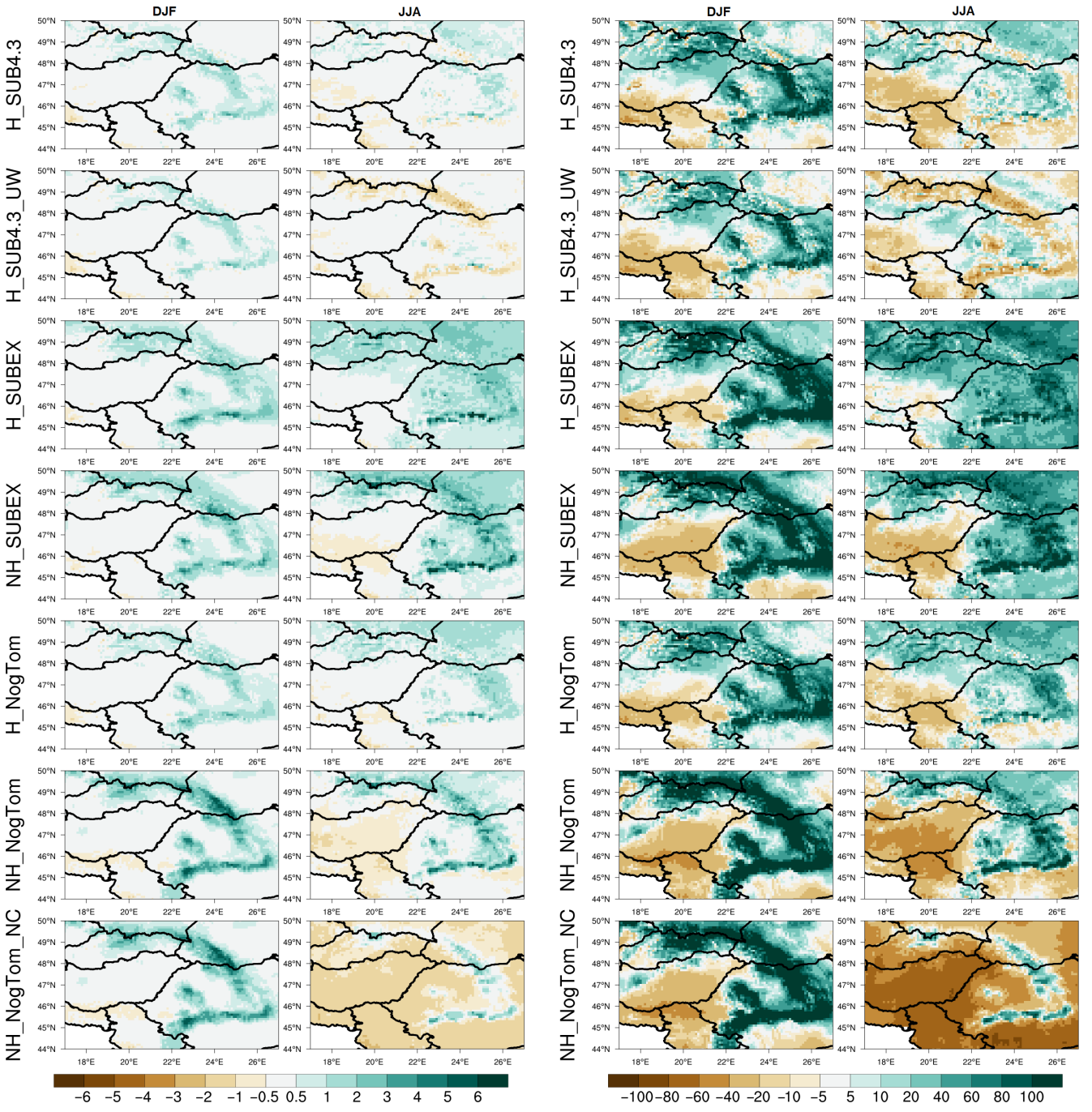

FIGURE 9 The winter and summer average precipitation bias (mm·day^{-1}) (left two columns) and winter and summer relative bias (%) (right two columns) of 10-km horizontal resolution RegCM simulations, 1981–1990 (validation data: CarpatClim)

diagrams in the central and right panels do not contain reference data. Moreover, the NH_NogTom_NC does not use convective parameterisation, therefore only total precipitation is given for that simulation.

Regarding the total precipitation, it can be seen that the H_SUB4.3 simulation overestimates the frequency of precipitation events over the subregions. Comparing the simulations, the H_NogTom captures the distribution of the CarpatClim data better, while the simulations that use the SUBEX scheme overestimate the high-intensity tail of the observed distribution. Overall, the NogTom scheme reproduces the observation better and the dynamical core does not have a substantial effect on the intensity of daily precipitation.

According to the PDF of the convective precipitation, as it can be seen in Figure 10, the highest frequency of

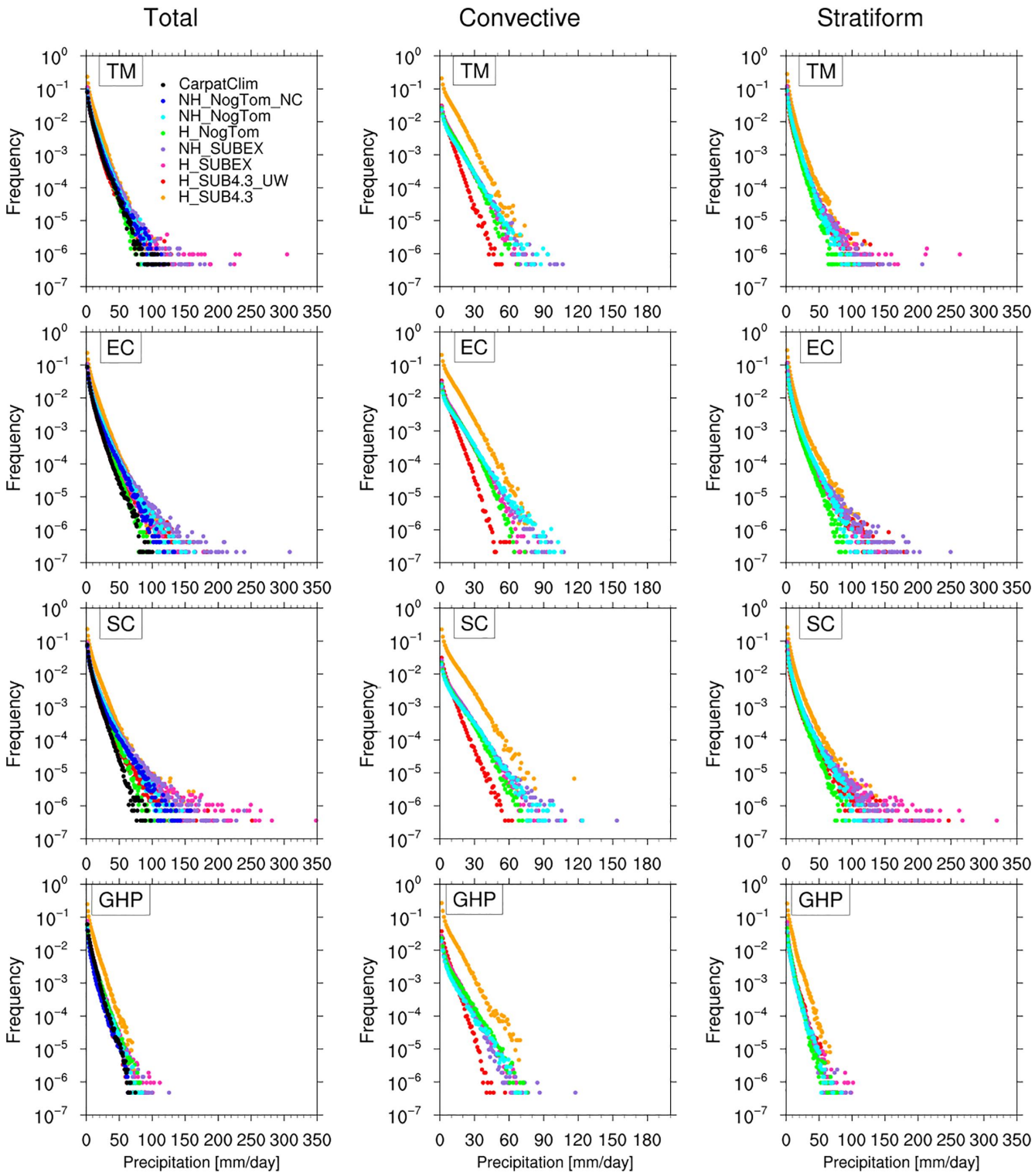

FIGURE 10 Daily precipitation intensity empirical probability distribution functions (PDFs) (frequency versus intensity of daily precipitation events, 1981–1990) for total, convective and stratiform precipitation over the four subregions

low intensity events occurs with the H_SUB4.3, while the simulation that uses the UW scheme has the lowest intensity over all subregions. These great differences do not occur in the total precipitation. On the basis of the presented results, the dynamical core does not have a noticeable effect on the moderate intensity events and we used the same convective parameterisation schemes in these simulations. The very high intensity events

(>80 mm·day^{-1}) occur only with a non-hydrostatic core, which certainly highlights the evident importance of a non-hydrostatic approach in reproducing intense convective precipitation events.

For stratiform precipitation, the simulations show similar results to those for total precipitation. The NogTom scheme causes the lowest frequency of precipitation events in general (especially when the intensity does not reach 80 mm·day^{-1}), while H_SUB4.3 has the highest frequency. In general, the high intensity events (>80 mm·day^{-1}) appear with SUBEX scheme, while the SUB4.3 moderates the occurrence of these events. Furthermore, the effect of UW scheme on the stratiform precipitation is lower than on the convective precipitation.

For a more detailed validation, we also evaluate how seasonal mean precipitation bias depends on elevation over the subregions (Figure 11). In winter the (mostly positive) biases are closer to zero over lower elevation areas (below 400 m) and no substantial differences can be seen between the simulations. The diagrams show that the biases grow and spread as elevation increases. Pronounced dependence on elevation can only be found in simulations using a non-hydrostatic core, and there is no substantial difference between the NH_NogTom and NH_NogTom_NC simulations. Furthermore, the SUB4.3 experiments perform better in all subregions and at all elevations in winter.

During the summer, the differences are more visible, more specifically the NH_NogTom_NC simulation underestimates the precipitation over lower elevations (below 400 m). Nevertheless, at higher elevations, larger negative biases appear with the H_SUB4.3_UW. It can also be seen that the NogTom simulations (except the NH_NogTom_NC) and the H_SUB4.3 resulted the smallest biases and the closest to zero in all subregions. Thus, the diagrams clearly suggest that the large scale precipitation scheme has a stronger effect on the dependence of elevation in summer precipitation bias than the effect of the dynamical core at this horizontal resolution.

3.5 | Comparison of Taylor diagram and DISO index

Taylor diagram (Figure 12) is analysed in this section and compared with the DISO index (Figure 13). Both metrics are used to investigate the temporal agreement between the simulated and observed fields, that is, the reproduction of annual variations. We used area-averaged monthly mean temperature, global radiation, cloud cover and precipitation fields for the subregions. On the basis of Figure 12, it can be concluded that the spatial averages of global radiation and temperature have the highest correlation rates (above 0.95) in all subregions. Regarding temperature, the H_SUB4.3_UW is the closest to the reference, especially over the lowland. In general, the other simulations overestimate temperature, as it was already shown in Figures 2 and 3. For global radiation, the correlation coefficients are high (above 0.95), and the standard deviation values are close to the CarpatClim data. Generally, the NH_NogTom_NC experiment underestimates the global radiation, which could be connected to the overestimation of cloud cover. This simulation does not use convective parameterisation, so only the dynamic core of the model produces precipitation, and convective precipitation is omitted, therefore substantial moisture remains in the clouds.

The results for cloud cover differ more from one simulation to the other, however most of the simulations underestimate cloud cover in all subregions. The NH_NogTom_NC resulted in the greatest differences from the reference since it does not capture the annual distribution of monthly average cloud cover, especially over mountainous areas. The selected subregions also affect the performance of simulations, namely, the NogTom scheme seems to be better over the mountainous area, while the H_SUB4.3_UW is better over lowland.

The lowest correlation rates appear with precipitation, which is one of the most varying variables in space and time, too. The lowest differences can be found between the individual experiments in monthly mean precipitation from a statistical point of view with the H_SUB4.3 simulation, where the standard deviation is very close to the measurements and the correlation coefficients are higher than 0.8. Despite the high correlation rates of simulations using the SUBEX scheme, these simulations also result in the highest standard deviations over the mountainous area. It is interesting that NH_NogTom is closer to the observation than H_NogTom despite the facts that NH_NogTom uses convective parameterisation and a non-hydrostatic core, too. The NH_NogTom_NC simulation underestimates precipitation the most, as it can be expected (and has already been shown in Figure 9).

The new measure DISO shows similar results for temperature as the Taylor diagram, namely the H_SUB4.3_UW seems to be the best (Figure 13). The modification of SUBEX does not result in any substantial improvement of DISO, since the original SUBEX has only slightly lower DISO values compared to SUB4.3 simulations. Furthermore, despite the general temperature overestimation shown in Figures 2–4, the experiments are better over lowlands than over mountainous areas from the overall aspect of DISO (i.e., DISO values for temperature are below 0.3 over lowlands and above 0.2 over

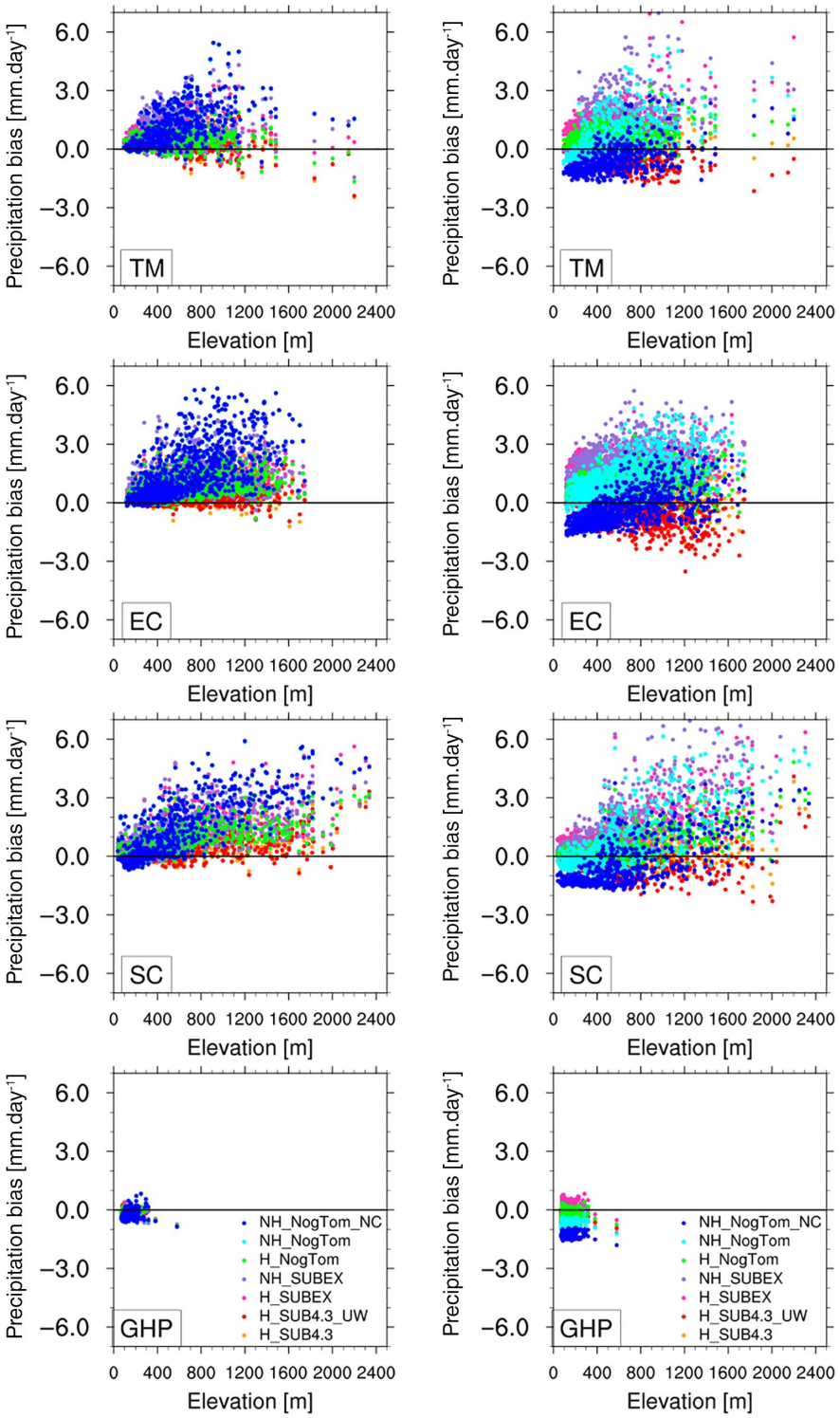

FIGURE 11 Elevation dependency of mean winter (left) and summer (right) precipitation over the four subregions

mountains in general, which is higher in the EC where it mostly exceeds 0.4). The NH_SUBEX results in the greatest DISO values for temperature over all subregions, which clearly imply that this simulation is not appropriate (similarly to the overall conclusion from Section 3.1).

The DISO values of global radiation are relatively low; the highest result is 0.2 implying a quite good overall reproduction of the statistical characteristics of observations despite the winter overestimations and summer underestimations (shown in Figure 6). Similarly to the conclusions in Section 3.2, DISO values in the selected subregions also confirm that the simulations using the modified SUBEX scheme (where the cloud-to-rain properties were adjusted) improve the overall performance. The NH_SUBEX results in the highest DISO values for global radiation, especially, in the TM where the

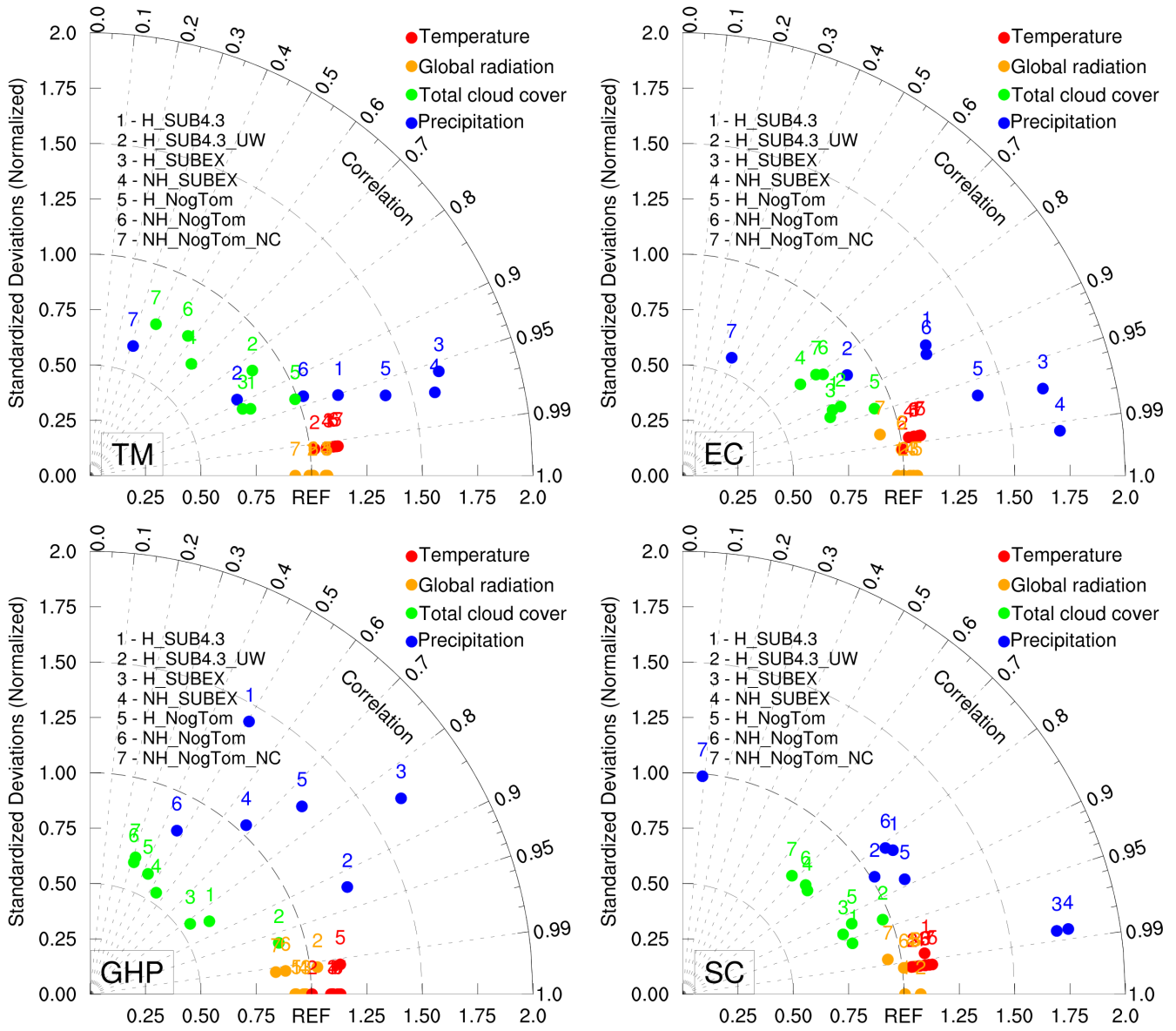

FIGURE 12 The Taylor diagrams of 10-km horizontal resolution RegCM simulations for monthly mean temperature, global radiation, cloud cover and precipitation totals for different subregions, 1981–1990

greatest summer bias is detected (as shown in Figure 6).

For the cloud cover, the DISO indicates differences in the subregional performance of individual simulations, namely, the NH_NogTom_NC is the least successful over the TM and the GHP, while the NH_SUBEX produces the highest DISO values over the two other subregions.

The biggest differences between the DISO values of individual simulations occur for precipitation similarly to the Taylor diagram (Figure 12). It is clear that the modified SUBEX scheme shows better performance in all subregions and the UW scheme slightly improves the results compared to the Holtslag scheme. Furthermore, the NogTom scheme is more appropriate regarding DISO values than the original SUBEX scheme in the case of either dynamical core. It is also clear that the H_NogTom simulation better reproduces the overall statistical characteristics of observed precipitation than the NH_NogTom as it can also be seen in Figure 8. The least successful simulation is obviously the NH_NogTom_NC, where the DISO values are the highest over all subregions. The worst DISO value (1.2) occurs over the SC region, which is probably due to the lack of precipitation stations (Szalai *et al.*, 2013), which would be necessary for a better representation of regional precipitation climatology in these elevated areas.

Overall, the modified SUBEX scheme results in lower DISO values for all variables and over all subregions,

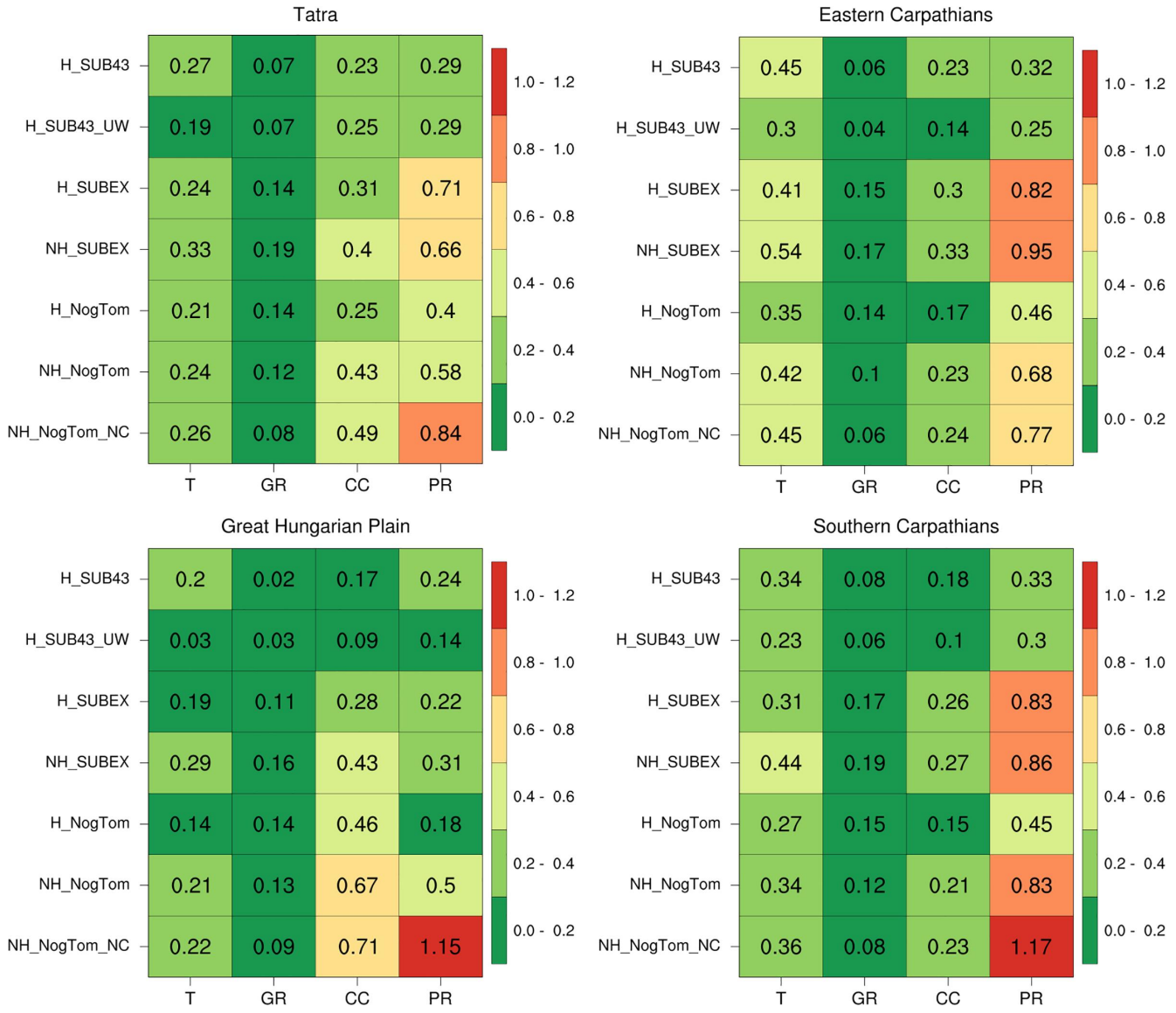

FIGURE 13 Evaluation of the RegCM simulations for monthly mean temperature (*T*), global radiation (GR), cloud cover (CC) and precipitation totals (PR) for different subregions using the DISO metric, 1981–1990

especially with the UW scheme. Differences between the conclusions from the Taylor diagram and DISO values are not substantial, nevertheless, it is advantageous to use both for the complete evaluation of results. On the basis of the results, DISO index can serve as a useful additional tool for the evaluation of climate simulations.

4 | CONCLUSIONS

This study aimed to evaluate RegCM4.5 simulations to determine whether they can be reliably used to further projection studies over the Carpathian region. The horizontal resolution of all the model experiments is 10 km, and decade-long (1981–1990) simulations have been conducted and analysed. RegCM4.5 includes the possible use of a non-hydrostatic dynamical core and an additional new microphysics scheme (NogTom). We also applied a modified version of the earlier large-scale precipitation scheme, which seemed to be more appropriate for this region (Torma *et al*., 2011); furthermore, we used two PBL schemes. The simulations were driven by ERA-Interim data for initial and boundary conditions. During validation we compared temperature, global radiation, cloud cover and precipitation with CarpatClim.

The seasonal mean climatological patterns of temperature are captured quite well by all model configurations and exhibit the spatial characteristics of CarpatClim. The H_SUB4.3_UW clearly improves the results, especially in summer, where the other simulations overestimate the

mean temperature by 3°C. More specifically, the UW scheme is characterized by a cooling effect due to the reduction of the eddy heat diffusivity in the lower troposphere, which occurs in this scheme.

For global radiation, not only the UW-PBL but also the modifications of SUBEX scheme result in the best reproduction of reference values. Although the UW scheme causes underestimation in winter, it reduces the bias over all regions better than the modified SUBEX scheme. This can be confirmed by the findings of Pieczka *et al*. (2019), namely, the UW scheme underestimates PBL height over the domain compared to the ERA-Interim, while the Holtslag scheme causes overestimation. In general, the overestimation occurs over the mountainous area, which is partially connected to the problem of the very few stations that perform actual global radiation measurements, and to the fact that this climatic element was computed from sunshine duration.

Most simulations overestimate cloud cover over the Carpathians in winter, while negative biases appear during summer. These negative biases clearly correlate to the overestimation of global radiation. Over lowland, negative biases are found in winter, which can be related to the fact that the model runs mostly ignore the foggy conditions obtained with the Holtslag scheme, and low level clouds are not treated properly.

In winter, all simulations overestimate precipitation, especially in the mountainous areas, and mostly the simulations that use a non-hydrostatic core. It can be concluded that the similarity between the NH_NogTom and NH_NogTom_NC in winter occurs because the convective parameterisation generally does not activate in winter in the target area, and thus, its effect remains negligible. Furthermore, the NH_NogTom_NC underestimates the summer precipitation over lowland, and a clear overestimation can be seen over mountains.

The main findings and conclusions can be summarized as follows:

1. The NogTom scheme improves the results over the Carpathian region compared to the SUBEX scheme, but this scheme is still worse than the SUB4.3 scheme.
2. The application of the SUB4.3 scheme decreases precipitation and cloud bias over all subregions.
3. The UW scheme reduces warm bias, despite causing a drier climate in summer.
4. The application of the SUB4.3 and UW schemes generally gives the best results in all climatic elements.
5. The role of the non-hydrostatic core can be clearly recognized for precipitation, particularly over the Carpathians.
6. Our validation results show that the overall best performance is achieved with H_SUB4.3_UW simulation for the Carpathian region.

In the light of the results, substantial effort is needed in the future, including a more extensive analysis of simulations (with the detailed evaluation of extreme events besides mean climatology), the implementation and testing of new physical processes in models, and more numerical experiments (with another land-surface model, with new convective schemes), to better understand and further improve climate models. Thus, the optimal model setup will be determined for the Carpathian region, which will be used for century-long simulations to assist the impact studies and decisions makers in developing mitigation and adaptation strategies on regional scale.

ACKNOWLEDGEMENTS

Research leading to this paper was supported by the following sources: the Széchenyi 2020 programme, the European Regional Development Fund and the Hungarian Government via the AgroMo project (GINOP-2.3. February 15, 2016-00028), the Hungarian National Research, Development and Innovation Fund under grants K-129162 and K-120605, and the Hungarian Ministry of Human Capacities under the ELTE Excellence Program (783-3/2018/FEKUTSRAT). Global reanalysis and model data used in this study were provided by the ECMWF. RegCM is distributed from the ICTP. CARPATCLIM Database European Commission – JRC, 2013.

ORCID

Tímea Kalmár https://orcid.org/0000-0003-0405-4404
Ildikó Pieczka https://orcid.org/0000-0001-5657-9494
Rita Pongrácz https://orcid.org/0000-0001-7591-7989

REFERENCES

Almorox, J. and Hontoria, C. (2004) Global solar radiation estimation using sunshine duration in Spain. *Energy Conversion and Management*, 45(9–10), 1529–1535. https://doi.org/10.1016/j.enconman.2003.08.022.

Ångström, A. (1924) Solar and terrestrial radiation. Report to the international commission for solar research on actinometric investigations of solar and atmospheric radiation. *Quarterly Journal of the Royal Meteorological Society*, 50(210), 121–126.

Bihari, Z., Babolcsai, G., Bartholy, J., Ferenczi, Z., Gerhátné Kerényi, J., Haszpra, L., Homoki-Ujváry, K., Kovács, T., Lakatos, M., Németh, Á., Pongrácz, R., Putsay, M., Szabó, P. and Szépszó, G. (2018) Climate. In: Kocsis, K. (Ed.) *National Atlas of Hungary: Natural Environment*. Budapest: MTA CSFK Geographical Institute, pp. 58–69.

Bretherton, C.S., McCaa, J.R. and Grenier, H. (2004) A new parameterization for shallow cumulus convection and its application

to marine subtropical cloud-topped boundary layers. Part I: description and 1D results. *Monthly Weather Review*, 132(4), 864–882. https://doi.org/10.1175/1520-0493(2004)132<0864:ANPFSC>2.0.CO;2.

Bucchignani, E., Montesarchio, M., Zollo, A.L. and Mercogliano, P. (2016) High-resolution climate simulations with COSMO-CLM over Italy: performance evaluation and climate projections for the 21st century. *International Journal of Climatology*, 36(2), 735–756. https://doi.org/10.1002/joc.4379.

Burk, S.D. and Thompson, W.T. (1989) A vertically nested regional numerical weather prediction model with second-order closure physics. *Monthly Weather Review*, 117(11), 2305–2324.

Ceglar, A., Croitoru, A.-E., Cuxart, J., Djurdjevic, V., Güttler, I., Ivančan-Picek, B., Jug, D., Lakatos, M. and Weidinger, T. (2018) PannEx: the Pannonian Basin experiment. *Climate Services*, 11, 78–85. https://doi.org/10.1016/j.cliser.2018.05.002.

Christensen, J.H., Boberg, F., Christensen, O.B., and Lucas-Picher, P. (2008) On the need for bias correction of regional climate change projections of temperature and precipitation. *Geophysical Research Letters*, 35(20), http://dx.doi.org/10.1029/2008gl035694.

Croitoru, A.-E., Piticar, A., Ciupertea, A.-F. and Roşca, C.F. (2016) Changes in heat waves indices in Romania over the period 1961–2015. *Global and Planetary Change*, 146, 109–121. https://doi.org/10.1016/j.gloplacha.2016.08.016.

Daly, C., Conklin, D.R. and Unsworth, M.H. (2009) Local atmospheric decoupling in complex topography alters climate change impacts. *International Journal of Climatology*, 30, 1857–1864. https://doi.org/10.1002/joc.2007.

Dee, D.P., Uppala, S.M., Simmons, A.J., Berrisford, P., Poli, P., Kobayashi, S., Andrae, U., Balmaseda, M.A., Balsamo, G., Bauer, P., Bechtold, P., Beljaars, A.C.M., van de Berg, L., Bidlot, J., Bormann, N., Delsol, C., Dragani, R., Fuentes, M., Geer, A.J., Haimberger, L., Healy, S.B., Hersbach, H., Hólm, E. V., Isaksen, L., Kållberg, P., Köhler, M., Matricardi, M., McNally, A.P., Monge-Sanz, B.M., Morcrette, J.J., Park, B.K., Peubey, C., de Rosnay, P., Tavolato, C., Thépaut, J.N. and Vitart, F. (2011) The ERA-interim reanalysis: configuration and performance of the data assimilation system. *Quarterly Journal of the Royal Meteorological Society*, 137(656), 553–597. https://doi.org/10.1002/qj.828.

Dickinson, R., Henderson-Sellers, A. and Kennedy, P. (1993) *Biosphere-atmosphere Transfer Scheme (BATS) Version 1e as Coupled to the NCAR Community Climate Model (p. 3040 KB)*. Boulder, Colorado: UCAR/NCAR. https://doi.org/10.5065/d67w6959.

Dickinson, R.E., Errico, R.M., Giorgi, F. and Bates, G.T. (1989) A regional climate model for the western United States. *Climatic Change*, 15(3), 383–422. https://doi.org/10.1007/BF00240465.

Elguindi, N., Bi, X., Giorgi, F., Nagarajan, B., Pal, J., Solmon, F., Rauscher, S., Zakey, A. and Giuliani, G. (2011) *Regional Climate Model RegCM User Manual Version 4.3*. Trieste: International Centre for Theoretical Physics (ICTP).

Elguindi, N., Bi, X., Giorgi, F., Nagarajan, B., Pal, J., Solmon, F., Rauscher, S., Zakey, A., O'Brien, T., Nogherotto, R. and Giuliani, G. (2014) *Regional Climate Model RegCM Reference Manual version 4.5*. Trieste: Abdus Salam ICTP, p. 33.

Emanuel, K.A. (1991) A scheme for representing cumulus convection in large-scale models. *Journal of the Atmospheric Sciences*, 48(21), 2313–2329. https://doi.org/10.1175/1520-0469(1991)048<2313:ASFRCC>2.0.CO;2.

Emanuel, K.A. and Živković-Rothman, M. (1999) Development and evaluation of a convection scheme for use in climate models. *Journal of the Atmospheric Sciences*, 56(11), 1766–1782. https://doi.org/10.1175/1520-0469(1999)056<1766:DAEOAC>2.0.CO;2.

Flato, G., Marotzke, J., Abiodun, B., Braconnot, P., Chou, S.C., Collins, W., Cox, P., Driouech, P., Emori, S., Eyring, V., Forest, C., Gleckler, P., Guilyardi, E., Jakob, C., Kattsov, V., Reason, C. and Rummukainen, M. (2013) Evaluation of climate models. In: Stocker, T.F., Qin, D., Plattner, G.-K., Tignor, M., Allen, S.K., Boschung, J., Nauels, A., Xia, Y., Bex, V. & Midgley, P.M. (Eds.) *Climate Change 2013: The Physical Science Basis. Contribution of Working Group I to the Fifth Assessment Report of the Intergovernmental Panel on Climate Change*. Cambridge, UK and New York, NY: Cambridge University Press, pp. 741–866. https://doi.org/10.1017/CBO9781107415324.020.

Fritsch, J.M. and Chappell, C.F. (1980) Numerical prediction of convectively driven mesoscale pressure systems. Part II. Mesoscale Model. *Journal of the Atmospheric Sciences*, 37(8), 1734–1762. https://doi.org/10.1175/1520-0469(1980)037<1734:NPOCDM>2.0.CO;2.

Gao, X., Xu, Y., Zhao, Z., Pal, J.S. and Giorgi, F. (2006) On the role of resolution and topography in the simulation of East Asia precipitation. *Theoretical and Applied Climatology*, 86(1–4), 173–185.

Geiger, R. (1951) The climate near the ground. *American Journal of Physics*, 19(3), 192–192.

Gibba, P., Sylla, M.B., Okogbue, E.C., Gaye, A.T., Nikiema, M. and Kebe, I. (2019) State-of-the-art climate modeling of extreme precipitation over Africa: analysis of CORDEX added-value over CMIP5. *Theoretical and Applied Climatology*, 137(1), 1041–1057. https://doi.org/10.1007/s00704-018-2650-y.

Giorgi, F., Coppola, E., Solmon, F., Mariotti, L., Sylla, M., Bi, X., Elguindi, N., Diro, G., Nair, V., Giuliani, G., Turuncoglu, U., Cozzini, S., Güttler, I., O'Brien, T., Tawfik, A., Shalaby, A., Zakey, A., Steiner, A., Stordal, F., Sloan, L.C. and Brankovic, C. (2012) RegCM4: model description and preliminary tests over multiple CORDEX domains. *Climate Research*, 52, 7–29. https://doi.org/10.3354/cr01018.

Giorgi, F. (1989) Two-dimensional simulations of possible mesoscale effects of nuclear war fires: 1. Model description. *Journal of Geophysical Research*, 94(D1), 1127. https://doi.org/10.1029/JD094iD01p01127.

Giorgi, F., Francisco, R. and Pal, J. (2003) Effects of a subgrid-scale topography and land use scheme on the simulation of surface climate and hydrology. Part I: effects of temperature and water vapor disaggregation. *Journal of Hydrometeorology*, 4(2), 317–333. https://doi.org/10.1175/1525-7541(2003)4<317:EOASTA>2.0.CO;2.

Giorgi, F., Solmon, F. and Giuliani, G. (2016a) Regional climatic model RegCM User's guide version 4.6 Trieste, Italy December 6, 2016, p. 57.

Giorgi, F., Torma, C., Coppola, E., Ban, N., Schär, C. and Somot, S. (2016b) Enhanced summer convective rainfall at alpine high elevations in response to climate warming. *Nature Geoscience*, 9 (8), 584–589.

Grell, G.A. (1993) Prognostic evaluation of assumptions used by cumulus parameterizations. *Monthly Weather Review*, 121(3), 764–787. https://doi.org/10.1175/1520-0493(1993)121<0764:PEOAUB>2.0.CO;2.

Grell, G.A., Dudhia, J. and Stauffer, D.R. (1994) *A Description of the Fifth-Generation Penn State/NCAR Mesoscale Model (MM5)*. Boulder: NCAR.

Güttler, I., Branković, Č., O'Brien, T.A., Coppola, E., Grisogono, B. and Giorgi, F. (2014) Sensitivity of the regional climate model RegCM4.2 to planetary boundary layer parameterisation. *Climate Dynamics*, 43(7–8), 1753–1772. https://doi.org/10.1007/s00382-013-2003-6.

Holtslag, A.A.M., De Bruijn, E.I.F. and Pan, H.-L. (1990) A high resolution air mass transformation model for short-range weather forecasting. *Monthly Weather Review*, 118(8), 1561–1575. https://doi.org/10.1175/1520-0493(1990)118<1561:AHRAMT>2.0.CO;2.

Hu, Z., Chen, X., Zhou, Q., Chen, D. and Li, J. (2019) DISO: a rethink of Taylor diagram. *International Journal of Climatology*, 39(5), 2825–2832.

Katragkou, E., García-Díez, M., Vautard, R., Sobolowski, S., Zanis, P., Alexandri, G., Cardoso, R.M., Colette, A., Fernandez, J., Gobiet, A., Goergen, K., Karacostas, T., Knist, S., Mayer, S., Soares, P.M.M., Pytharoulis, I., Tegoulias, I., Tsikerdekis, A. and Jacob, D. (2015) Regional climate hindcast simulations within EURO-CORDEX: evaluation of a WRF multi-physics ensemble. *Geoscientific Model Development*, 8(3), 603–618. https://doi.org/10.5194/gmd-8-603-2015.

Kotlarski, S., Keuler, K., Christensen, O.B., Colette, A., Déqué, M., Gobiet, A., Goergen, K., Jacob, D., Lüthi, D., van Meijgaard, E., Nikulin, G., Schär, C., Teichmann, C., Vautard, R., Warrach-Sagi, K. and Wulfmeyer, V. (2014) Regional climate modeling on European scales: a joint standard evaluation of the EURO-CORDEX RCM ensemble. *Geoscientific Model Development*, 7 (4), 1297–1333. https://doi.org/10.5194/gmd-7-1297-2014.

Nogherotto, R., Tompkins, A.M., Giuliani, G., Coppola, E. and Giorgi, F. (2016) Numerical framework and performance of the new multiple-phase cloud microphysics scheme in RegCM4.5: precipitation, cloud microphysics, and cloud radiative effects. *Geoscientific Model Development*, 9(7), 2533–2547. https://doi.org/10.5194/gmd-9-2533-2016.

O'Brien, T.A., Chuang, P.Y., Sloan, L.C., Faloona, I.C. and Rossiter, D.L. (2012) Coupling a new turbulence parametrization to RegCM adds realistic stratocumulus clouds. *Geoscientific Model Development*, 5(4), 989–1008. https://doi.org/10.5194/gmd-5-989-2012.

Pal, J.S., Small, E.E. and Eltahir, E.A. (2000) Simulation of regional-scale water and energy budgets: representation of subgrid cloud and precipitation processes within RegCM. *Journal of Geophysical Research: Atmospheres*, 105(D24), 29579–29594.

Pieczka, I., Pongrácz, R., Németh, C.P. and Kalmár, T. (2019) Analysis of regional climate model simulations for Central Europe as a potential tool to assess weather-related air quality conditions. *International Journal of Environment and Pollution*, 66 (1–3), 98–116. https://doi.org/10.1504/IJEP.2019.104524.

Pieczka, I., Pongrácz, R., Szabóné André, K., Kelemen, F.D. and Bartholy, J. (2017) Sensitivity analysis of different parameterization schemes using RegCM4.3 for the Carpathian region. *Theoretical and Applied Climatology*, 130(3–4), 1175–1188. https://doi.org/10.1007/s00704-016-1941-4.

Prescott, J. (1940) Evaporation from a water surface in relation to solar radiation. *Transactions. Royal Society of South Australia*, 46, 114–118.

Sinha, P., Mohanty, U.C., Kar, S.C., Dash, S.K. and Kumari, S. (2013) Sensitivity of the GCM driven summer monsoon simulations to cumulus parameterization schemes in nested RegCM3. *Theoretical and Applied Climatology*, 112(1–2), 285–306. https://doi.org/10.1007/s00704-012-0728-5.

Spinoni, J., Antofie, T., Barbosa, P., Bihari, Z., Lakatos, M., Szalai, S., Szentimrey, T. and Vogt, J. (2013) An overview of drought events in the Carpathian region in 1961–2010. *Advances in Science and Research*, 10(1), 21–32. https://doi.org/10.5194/asr-10-21-2013.

Spinoni, J., Lakatos, M., Szentimrey, T., Bihari, Z., Szalai, S., Vogt, J. and Antofie, T. (2015a) Heat and cold waves trends in the Carpathian region from 1961 to 2010. *International Journal of Climatology*, 35(14), 4197–4209. https://doi.org/10.1002/joc.4279.

Spinoni, J., Szalai, S., Szentimrey, T., Lakatos, M., Bihari, Z., Nagy, A., Németh, Á., Kovács, T., Mihic, D., Dacic, M., Petrovic, P., Kržič, A., Hiebl, J., Auer, I., Milkovic, J., Štepánek, P., Zahradnícek, P., Kilar, P., Limanowka, D., Pyrc, R., Cheval, S., Birsan, M.V., Dumitrescu, A., Deak, G., Matei, M., Antolovic, I., Nejedlík, P., Štastný, P., Kajaba, P., Bochnícek, O., Galo, D., Mikulová, K., Nabyvanets, Y., Skrynyk, O., Krakovska, S., Gnatiuk, N., Tolasz, R., Antofie, T. and Vogt, J. (2015b) Climate of the Carpathian region in the period 1961-2010: Climatologies and trends of 10 variables. *International Journal of Climatology*, 35(7), 1322–1341. https://doi.org/10.1002/joc.4059.

Stadtherr, L., Coumou, D., Petoukhov, V., Petri, S. and Rahmstorf, S. (2016) Record Balkan floods of 2014 linked to planetary wave resonance. *Science Advances*, 2(4), e1501428. https://doi.org/10.1126/sciadv.1501428.

Sundqvist, H., Berge, E. and Kristjánsson, J.E. (1989) Condensation and cloud parameterization studies with a mesoscale numerical weather prediction model. *Monthly Weather Review*, 117(8), 1641–1657. https://doi.org/10.1175/1520-0493(1989)117<1641:CACPSW>2.0.CO;2.

Szalai, S., Auer, I., Hiebl, J., Milkovich, J., Radim, T., Stepanek, P., Zahradnicek, P., Bihari, Z., Lakatos, M., Szentimrey, T., Limanowka, D., Kilar, P., Cheval, S., Deak, Gy., Mihic, D., Antolovic, I., Mihajlovic, V., Nejedlik, P., Stastny, P., Mikulova, K., Nabyvanets, I., Skyryk, O., Krakovskaya, S., Vogt, J., Antofie, T. and Spinoni, J. (2013) Climate of the Greater Carpathian Region. *Final Technical Report*. www.carpatclim-eu.org.

Taylor, K.E. (2001) Summarizing multiple aspects of model performance in a single diagram. *Journal of Geophysical Research: Atmospheres*, 106(D7), 7183–7192. https://doi.org/10.1029/2000JD900719.

Tiedtke, M. (1993) Representation of clouds in large-scale models. *Monthly Weather Review*, 121(11), 3040–3061. https://doi.org/10.1175/1520-0493(1993)121<3040:ROCILS>2.0.CO;2.

Tompkins, A.M., Gierens, K. and Rädel, G. (2007) Ice supersaturation in the ECMWF integrated forecast system. *Quarterly Journal of the Royal Meteorological Society*, 133(622), 53–63. https://doi.org/10.1002/qj.14.

Torma, C., Coppola, E., Giorgi, F., Bartholy, J. and Pongrácz, R. (2011) Validation of a high-resolution version of the regional climate model RegCM3 over the Carpathian Basin. *Journal of Hydrometeorology*, 12(1), 84–100. https://doi.org/10.1175/2010JHM1234.1.

Velikou, K., Tolika, K., Anagnostopoulou, C. and Zanis, P. (2019) Sensitivity analysis of RegCM4 model: present time simulations over

the Mediterranean. *Theoretical and Applied Climatology*, 136(3–4), 1185–1208. https://doi.org/10.1007/s00704-018-2547-9.

WMO. (2007) *The Role of Climatological Normals in a Changing Climate (WMO-TD no. 1377/WCDMP-No. 61)*. Geneva, Switzerland: WMO.

Xu, Z. and Han, Y. (2019) Comments on 'DISO: a rethink of Taylor diagram'. *International Journal of Climatology*, 40, 2506–2510. https://doi.org/10.1002/joc.6359.

How to cite this article: Kalmár T, Pieczka I, Pongrácz R. A sensitivity analysis of the different setups of the RegCM4.5 model for the Carpathian region. *Int J Climatol*. 2021;41 (Suppl. 1): E1180–E1201. https://doi.org/10.1002/joc.6761